NUCLEAR SPECTROSCOPY STUDIES IN Xe^{131m} AND Sb^{125}

By

ALI A. ABDULLA

Bachelor of Science
University of Baghdad
Baghdad, Iraq
1961

Master of Science
University of Notre Dame
South Bend, Indiana
1964

Submitted to the faculty of the Graduate College
of the Oklahoma State University
in partial fulfillment of the requirements
for the Degree of
DOCTOR OF PHILOSOPHY
May, 1969

NUCLEAR SPECTROSCOPY STUDIES

IN Xe^{131m} AND Sb^{125}

Thesis Approved:

N. V. V. J. Swamy
Thesis Adviser

Melvin J. Fischbach

Leon W. Schroeder

Lionel M. Raff

D. D. Durham
Dean of the Graduate College

PREFACE

Earlier attempts to detect a second order transition in some isomeric nuclei have, while being somewhat successful, shown discrepancies between theoretical estimates and experimental results. The experimental results and their interpretation, as performed by different groups, have been rather conflicting. Especially in Xe^{131m} there are two different reported results with two different interpretations of the observed effect. Due to this discrepancy a need existed for further investigations. It is the hope of the author that the results obtained herein may be helpful in resolving the existing conflict.

The author wishes to express his sincere gratitude to Dr. N. V. V. J. Swamy, his thesis adviser, and Dr. H. J. Fischbeck of the University of Oklahoma for their invaluable assistance and guidance in this work, Dr. H. E. Harrington, ex-Head of the Physics Department, for his kind help and to the Government of Iraq for the opportunity given to him to do his advanced studies in the U. S. A.

TABLE OF CONTENTS

LIST OF TABLES

LIST OF FIGURES

CHAPTER I

INTRODUCTION

When a nucleus is in an excited state, the usual process under which it de-excites itself is the emission of a single quantum, either a photon or an electron. Another possible process is the so-called second order process,* the emission of double quanta. In this process the nucleus is de-excited with the emission of two quanta--two photons, two electrons or one of each--and these two quanta share the total available energy in a continuous way, a feature which characterizes this process and could be used as its distinguishing mode.

It is of interest to know the ratio between the transition probabilities of the second and first order type of de-excitation of nuclear states. The theoretical treatment of the double quantum emission has been carried out by many authors[1,2,3,4] since the thirties, but as yet there is no unqualified experimental confirmation of the theoretical predictions. The difficulties involved in studying this second order process are due to the fact that it is a very weak effect and it is usually masked by the much more common first order processes. It, therefore, seems natural to study this phenomenon by using some coincidence technique.

---

*There can also be a first order transition, but this is usually several orders of magnitude weaker than the second order one. This point will be discussed later.

Since the second order process is so weak and cannot compete with the first order one or the single transition, one has to search for decays in which the first order process is hindered. One of these cases is the one in which the double quantum emission occurs as a result of a transition of high multipolarity. Furthermore, it will be favorable and easier if the decay contains only two levels with electro magnetic transition between them. Then the possibility for detection depends on how favorable the ratio is between the transition probabilities for double and single quantum emission and these are mainly due to the spins and parities of the initial and final states in the nucleus. Eichler et al,[3] using the single particle model, calculated the ratio between the transition probabilities of double and single quantum emission approximately as,

$$\frac{P_{\gamma\gamma}(L,\ L')}{P_{\gamma}(L_o)} = \frac{1}{137}\left(\frac{1}{2}\right)^{2L_o+2}\ ;\quad (L_o \geq 2\ ;\ L + L' = L_o)$$

where L, L' are the multiple orders of the double quantum transitions and L_o is the multiple order of the single quantum transition.

Thus one finds that Xe^{131m} is a good case to detect the second order process, in as much as it has an isomeric level $h_{11/2}$ and the level to which it decays is lower in angular momentum by several units. It has a half-life of 12 days and it decays to the ground state, which is $d_{3/2}^{+}$, by a 164 M4 transition. The double photon decay is expected to accompany this M4 gamma transition. The probability of the double quantum emission in Xe^{131m} will be measured by observing the coincidence rate between the two X-rays which result from the internal conversion of the two gamma quanta. The result of the coincidence between these

two X-rays will be observed as a line instead of a broad continuum, a condition which is more favorable in studying a small effect phenomenon.

In the last few years a great improvement has been introduced into the experimental technique, especially the advances made in the building of high resolution solid state detectors and in the sophistication of coincidence techniques. These developments make it, hopefully, possible to search for the double quantum emission in some of the simple observable decay cases and Xe^{131m} is one of them. Ever since Mize et al's[5] experiments in Ir^{192m} many workers have been searching for the detection of the second order effects, $\gamma\gamma$, γe, or ee.

Vanderleeden and Jastram[6] investigated the double quantum emission accompanying the 1.76 Mev transition in Zr^{90}. Their result places an upper limit of 8.10^{-5} on the ratio of the transition probabilities for the second order process and the first order modes. Very recently, Church and Gerholm[7] made their observations on the decay of In^{119m}. Their results show no evidence for double K-electron emission, but an upper limit on double quantum emission was reported as $\gamma\gamma/\gamma < 3.10^{-4}$. Ga^{40} was investigated, independently, by Nessin et al[8] and Dell et al.[9] In this case the 3.35 Mev transition takes place from the level 0^+ to the level 0^+, where first order processes are absolutely forbidden. The reported result gives an upper limit of about 10^{-2} for double quantum emission. Alvager et al[10] have searched for the double quantum emissions which compete with M2 transition in K^{41} and Rb^{85}. Their results place an upper limit for the ratio between the probability for double quantum emission, $\gamma\gamma$, and the probability for single quantum emission, γ, in the limit of $\frac{\gamma\gamma}{\gamma} < 6.10^{-5}$ and $\frac{\gamma\gamma}{\gamma} < 1.2.10^{-5}$ for the

1.29 Mev level in K^{41} and for the 0.514 Mev level in Rb^{85}, respectively. The double quantum emission which is competing with the M4 transition in Xe^{131m} was investigated by Alvager et al[11] in 1960. Use of two NaI crystals was made with a tube type multichannel analyzer and a conventional fast-slow coincidence unit. They reported that the double quantum emission to the single ratio is about 8.10^{-4} for E2 M2 transition type and 10^{-4}, 10^{-5} for E3 M1 and E1 M3 respectively. These values were based on the coincidence counts under the X-ray peak in the coincidence spectrum. However, Listengarten,[14] in his theoretical formula for the double K-electron conversion ratio, showed that the reported result by reference[11] is more likely to be the $\frac{W_{kk}}{W_k}$, double K-electron conversion to the K-electron conversion ratio. On the other hand, Knauf et al[12] re-investigated the Xe^{131m} case using two NaI crystals and in conjunction with a two-dimensional energy analysis. Their results give an upper limit of $2.2.10^{-5}$ for the ratio of the $\gamma\gamma$- to γ-transition and $(3.6\pm0.7).10^{-3}$ for the double K-electron emission to γ emission probability. In addition to that they measured the K-conversion coefficient and the half-life of Xe^{131m} to be 32.1 ± 0.4 and 11.99 ± 0.04d, respectively. They, also, attribute the continuum following the X-ray peak in the coincidence spectrum to the external Bremsstrahlung, a point which contradicts the result of reference.[11] Because of these conflicting experiments, it was considered worth while to re-investigate this case with the high resolution solid state detector and possibly resolve the discrepancy in the reported results.

In the decay of Sb^{125} there exists a controversy about the spin assignment of a level at 0.321 Mev in Te^{125} which is the product of the decay. The experimental work of Narcisi[19] assigns a spin of 9/2

and odd parity whereas the theoretical work of Glendenning[22] contradicts this. A group in India reported a level at 0.401 Mev which has not been confirmed by others. These points can be settled by a precise measurement of the energy levels using solid state detectors and also angular correlation measurements. This was undertaken and this work forms the second part of the thesis.

CHAPTER II

THEORY OF DOUBLE QUANTUM EMISSION

The usual mode of decay of an excited nucleus to its ground state is by the emission of a single quantum of multipolarity $\vec{L}_o = \vec{j}_i - \vec{j}_f$ ($|j_i - j_f| \leq j_i + j_f$), $\pi_i \pi_f = (-1)^{L_o}$. The angular momentum and corresponding projection quantum numbers of initial and final states of the nucleus are denoted by $j_i \mu_f$ and $j_f \mu_f$ respectively. Their parities will be denoted by $\pi_i \pi_f$ and + is even parity and - odd parity. If one quantum of order L_o is replaced by two quanta of order L and L′ ($E_i - E_f = \hbar\omega$, $\hbar\omega_1 + \hbar\omega_2 = \hbar\omega$), then the inequality satisfied is $|L - L'| \leq L_o \leq L + L'$. However, in some cases a simultaneous emission of two quanta is quite possible. These processes, from a quantum mechanical point of view, are called first and second order processes respectively. Assuming the angular momentum is conserved in the transition, Table I lists the possible multipolarities of $\gamma\gamma$ and γ decays. In addition to two photon emission other possible two quantum emissions are: (a) X-ray and an electron (γe process), or (b) two converted electrons (ee). Schwinger and Oppenheimer[13] considered the two photon transition of the type E1E1. A Case of particular interest is the 0 - 0 angular momentum transition because here the one photon decay mode is structly forbidden. Sachs[2] evaluated the probabilities for the $\gamma\gamma$ and γe processes in $0^+ \rightarrow 0^-$ transition. The Schrodinger equation for the motion of a particle of mass m and the charge e in an electro-

magnetic field described by the potentials A and Φ, with an additional potential V, is given

$$i\hbar\frac{\partial\psi}{\partial t} = \left[-\frac{\hbar^2}{2m}\nabla^2 + \frac{ie\hbar}{mc}\vec{A}\cdot\vec{\nabla} + \frac{ie\hbar}{2mc}\vec{\nabla}\cdot\vec{A} + \frac{e^2}{2mc^2}A^2 + e\Phi + V\right]\psi \qquad (1)$$

A and Φ represent an electromagnetic field that is weak enough so that those terms containing A and Φ can be regarded as a perturbation. V is the potential energy that binds the particle.

Tha Hamiltonian of one particle interacting with an external electromagnetic field discribed by the potentials A and Φ is

$$H = -\frac{\hbar^2}{2m}\nabla^2 + \frac{ie}{mc}\vec{A}\cdot\vec{\nabla} + \frac{ie\hbar}{2mc}\vec{\nabla}\cdot\vec{A} + e\Phi + V \qquad (2)$$

With Coulomg-gauge $\vec{\nabla}\cdot\vec{A} = \Phi = 0$, Eq. (2) is reduced to

$$\begin{aligned} H &= \frac{-\hbar^2}{2m}\nabla^2 + \frac{ie\hbar}{mc}\vec{A}\cdot\vec{\nabla} + \frac{e^2}{2mc^2}A^2 + V \\ &= H_o + H' \end{aligned} \qquad (3)$$

where $H_o = \frac{-\hbar^2}{2m}\nabla^2 + V$, the Hamiltonian of the system when there is no perturbing field, $H' = \frac{ie\hbar}{mc}\vec{A}\cdot\vec{\nabla} + \frac{e^2}{2mc^2}A^2$, the perturbation term. The Hamiltonian in Eq. (3) is true only if there is no interaction between the field and the spin of the particle. Including spin interactions, we have in the non-relativistic case

$$H = H_o + \frac{ei\hbar}{mc}\vec{A}\cdot\vec{\nabla} + \frac{e^2}{2mc^2}A^2 - \mu\frac{e\hbar}{2mc}\vec{\sigma}\cdot\vec{\nabla}\times\vec{A} \qquad (4)$$

where H' (perturbation term) becomes

$$H' = \frac{ei\hbar}{mc}\vec{A}\cdot\vec{\nabla} + \frac{e^2}{2mc^2}A^2 - \mu\frac{e\hbar}{2mc}\vec{\sigma}\cdot\vec{\nabla}\times\vec{A} \qquad (5)$$

$\vec{\sigma}$ is the Pauli operator which is related to spin operator as

$$\vec{S} = \frac{\hbar}{2}\vec{\sigma} \qquad (6)$$

μ is the magnetic moment of the particle. Since the nucleus contains as many nucleons as its mass number A, the H' in Eq. (5) can be written for the system as

$$H' = \sum_{i=1}^{A} \frac{eih}{mc} \delta i(\vec{A}(r_i)\cdot\vec{\nabla}) - \sum_{i=1}^{A} \mu_i \frac{eh}{2mc} \vec{\sigma}\cdot\vec{\nabla} \times \vec{A}(r_i) + \frac{e^2}{2mc^2} \sum_{i=1}^{A} A^2(r_i) \qquad (7)$$

where $\delta_i = 1$ for protons and $\delta_i = 0$ for neutrons. By applying perturbation theory one can calculate the transition probability for first or second order processes (two photon, two electron or photon and electron). The transition probability, in general, is given by

$$T_{n\to m} = \frac{2\pi}{\hbar} \left| H'_{nm} \right|^2 P(E) \qquad (8)$$

where P(E) is the final state density and $\bar{H}nm$ is the matrix element of the perturbing Hamiltonian between the states n and m of the nuclear system making the transition. A direct transition $i \to f$ gives second order effect as far as the A^2 term is concerned. But the term linear in A leads to second order transitions only when intermediate states are involved, i.e., $i \to I \to f$. It turns out, however, the A^2 term is several orders of magnitude less than the other term and is, hence, neglected in almost all calculations.

The multipole selection rule arises out of the usual representation of the vector potential $\vec{A} = \mu_p(\hat{k})e^{i\vec{K}.\vec{r}}$ where μ_p is a polarization vector and $\vec{K}$ the wave vector. The plane wave $e^{i\vec{K}.\vec{r}}$ is decomposed into angular momentum waves (multipole decomposition)

$$\vec{A} = \sum_{L} \vec{A}(EL) + \vec{A}(ML)$$

The corresponding terms in each summation have opposite parities.

Formula 8 shows clearly that the detailed transition probability depends on the nuclear model used which governs the matrix element $\bar{H}nm = \langle n|\bar{H}|m\rangle$. Mayer[1] was the first one to consider quantum mechanically second order transition probabilities. Using only the dipole approximation, she calculated the transition probability for double quantum emission in atoms. In her calculation she did not include the interaction between particle spin and the electromagnetic field. Sachs[2] essentially used Mayer's transition probabilities for his $e\gamma$ predictions. The generalization of Mayer's results to higher multipoles, as also taking the spin into account, was done by Eichler and Jacob[3] who concentrated on the application of these processes to nuclei. One important contrast between atoms and nuclei is the fact that in the latter case one encounters angular momentum differences of several units (specially in isomers) and hence higher multipolarities are important. They also considered the case $0^+ \rightarrow 0^-$ transitions where first order processes are completely forbidden.

At this stage a discussion of the angular momentum selection rules is in order. Because of the fact that the multipole fields have definite angular momentum and parity and these are conserved in electromagnetic decays, we have the result that, in a single quantum emission or multipolarity L_0 due to a nuclear transition from state i to state f we have

$$|j_i - j_f| \leq L_o \leq j_i + j_f$$

$$\pi_i\pi_f = (-1)^{L_o}\,(EL_o)$$

$$= (-1)^{L_o+1}\,(ML_o)$$

the electric multipoles have parity $(-1)^{L_o+1}$ and magnetic multipoles have parity $(-1)^{L_o}$.

Table I summarizes the allowed single and corresponding double quantum transitions:

TABLE I

MULTIPOLARITIES OF SINGLE QUANTUM AND COMPETING DOUBLE QUANTUM TRANSITION

Single Quantum	Double Quantum ($\gamma\gamma$).
E2	(E1E1), (M1M1).
E3	(E1E2), (M1E2).
E4	(E1E3), (E2E2), (M1M3), (M2M2).
E5	(E1E4), (E2E3), (M1M4), (M2M3).
M2	(E1M1).
M3	(E2M1), (E1M2).
M4	(E1M3), (E2M2), (E3M1).
M5	(E1M4), (E2M3), (E3M2), (E4M1).

In the case of double quantum emission, if we denote the energies and angular momenta of these two gamma rays by $\hbar W$ and $\hbar W'$, L and L′ respectively, it is clear that L, L′ and L_o have to satisfy the quantum mechanical angular momentum addition rule. Conservation of energy requires $\hbar\omega = \hbar\omega + \hbar\omega' = \hbar\omega_i - \hbar\omega_f$. The following energy level diagram summarizes notations.

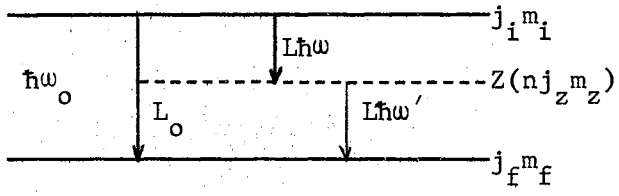

For the special case $L + L' = L_o = |j_i - j_f|$ and assuming that a single particle in the nucleus, the state of which is described by the quantum numbers n, j, l, m, makes the transition i to f, Eichler and Jacob[3] derived the following formula for a two quantum emission:

$$T_{\gamma\gamma}d\omega = \frac{8}{\pi}d\omega\left(\frac{e^2}{\hbar c}\right)^2\left(\frac{\hbar}{mc}\right)^4 \omega\omega' \frac{2j_f + 1}{2j_i + 1}\sum \frac{1}{(2L + 1)(2L' + 1)} x$$

$$x \left\{ \sum_M \frac{\langle f\|T_L^{\tau'}(k)\|z\rangle \langle z\|T_L^{\tau}(k)\|i\rangle}{w_i - w_z - w} \sum_{n'} \frac{\langle f\|T_L^{\tau}(k)\|z'\rangle \langle z\|T_L^{\tau'}(k')\|1\rangle}{w_i - w_{z'} - w'} \right\} \tag{19}$$

Here M is the mass of the nucleon, $\langle f \|T_L^{\tau}\| i\rangle$ are the reduced matrix elements of the (electric or magnetic multipole τ = el or mag) irreducible tensor operator T_L^{τ} pertaining to the multipole decomposition of the electromagnetic field and z specifies an intermediate state with quantum numbers n, j, l, m and energy $\hbar\omega'$. From this formula, using the model of an isotropic harmonic oscillator without spin orbit coupling for the single particle, they make an approximate estimate of the ratio of the two quantum to single gamma transition as $\frac{T(L,L')}{T(L_o)} = \frac{1}{137} \cdot (\tfrac{1}{2})^{2L_o+2}$. Eichler extended these calculations and gave approximate estimates for $T_{\gamma e_k}$ and $T_{e_k e_k}$. He finds that $T_{e_k e_k}$ is larger than $T_{\gamma\gamma}$ by an order of magnitude.

The isomer Xe^{131m} is a nucleus with 4 units of angular momentum

difference between the metastable state and ground state. It has a half-life of 12 days. Its single quantum decay is illustrated in the following:

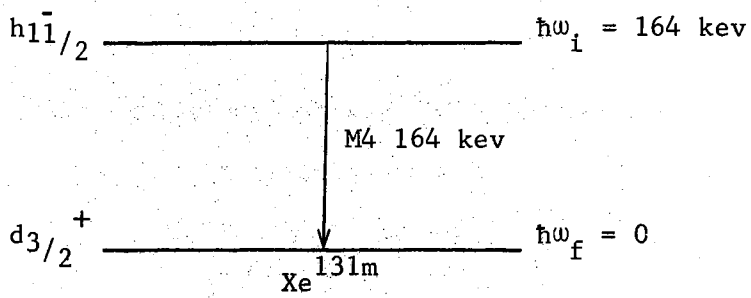

For this nucleus Eichler and Jacob estimate the ratio of double quantum to single quantum transition as

$$\frac{T_{\gamma\gamma}(L,L')}{T_{\gamma\gamma}(L_o)} \cong 5.10^{-5}$$

Because of the following approximations the results of Eichler and Jacob are usually considered only as rough estimates:

a) a single particle model of a harmonic oscillator without spin orbit coupling is used for the nucleus in the evaluation of the nuclear matrix element $\langle n|\bar{H}|m\rangle$.

b) only one or two intermediate states are considered.

c) the multipolarity of the radiation is restricted to the case $L + L' = L_o$.

d) in the case of 0 - 0 transitions the single quantum energy is assumed to be equally divided between the two quanta in the double quantum transition.

e) other numerical approximations including the assumption that the matrix elements are weakly dependent on the energies of

the quanta.

Furthermore in their analysis it turns out that the quantum spectrum depends on the parities as well as the multipolarities of the two quanta, in contradiction to the conclusions of Sachs and Schwinger.[2,13] An improvised treatment has been made by Grechukin[4] who starts with a many particle Hamiltonian. His estimate is given by the formula

$$\frac{T_{\gamma\gamma}(L,L')}{T_{\gamma}(L)} \cong (5 \text{ to } 1)\cdot 10^{-5} \times \left\{\frac{W_o^{\,2}\Phi(L_o L' L;\ j_i j_f)}{|\langle j_f \| L \| \delta_i \rangle|^2}\right\} \qquad (10)$$

the factor in braces depends on the nuclear model. The numerical factor emerges out of angular integrations involved in assuming the applicability of Racah algebra. When the energy of the single quantum is unequally distributed between the two quanta there is a likelihood of interference in the probabilities of emission of these latter two quanta. Assuming a cancellation of these interference terms (random phase approximation), using the model of an independent particle model with spin orbit coupling and a phenomenological model of quadrupole collective nuclear excitations background, Grechukin estimates

$$\frac{T_{\gamma\gamma}}{T_{\gamma}(M3)} \simeq 1.8\cdot 10^{-5} \text{ in } Cl^{38}$$

While we shall postpone a detailed comparison of theory and experiment to a later chapter one point has to be mentioned here. In the actual experiment, what is usually observed is a coincidence between two X-rays resulting from the escape of two K electrons which is due to the internal conversion of the two gamma rays in the ground state transition of Xe^{131m}. There can be an alternative interpretation of this experimental observation as was pointed out by Listengarten.[14]

In a process of internal Compton effect the nucleus emits a virtual photon in a transition and this virtual photon makes a Compton collision with one of the K electrons resulting in a real photon and the emission of an electron. It is quite possible that, in the experiment studied, the second electron is due to the internal conversion of this real photon, and thus instead of saying double internal conversion due to double quantum emission one can as well say double electron emission following an internal Compton effect. Jacobson[15] worked out the theory of internal Compton effect. Based on this Listengarten calculates for small transition energies the probability of double conversion in the K shell as approximately equal to the probability of internal Compton effect in the K shell multiplied by the internal conversion coefficient of the multipole radiation:

$$\frac{W_{kk}}{W_k} = \frac{4\alpha}{3} W \int_{k_i}^{k_2} \frac{dk}{k} \cdot \frac{1}{2} \alpha_k^{(1)}(k,z) \qquad (11)$$

Here W_k and W_{kk} are emission probabilities of one and two K electrons, α is the Sommerfeld fine structure constant and W is the transition energy in units of mc^2. $\alpha k_1 = \Sigma_k$, $k_2 = W - \Sigma_k$ and Σ_k is the binding energy of K electrons. α_k is the conversion coefficient in the K shell. If we substitute W = .322, Σ_k = .068 and .089 $\leq \alpha_k \leq$ 2.22, corresponding to the experimental situation in Xe^{131m}, eq. (11) then gives a numerical value 5.0×10^{-4} for the ratio of double conversion to single conversion probability in Xenon.

CHAPTER III

EXPERIMENTAL TECHNIQUE AND METHODS

Preparation of the Sample

The sample of Xe^{131m} was prepared in the following steps:

1. I^{131} carrier free was brought in the chemical form of Ino·1N NaoH and its radiochemical purity was 99%. It is well known that I^{131} has a half-life of 8 days and it decays by β^- to Xe^{131} (See Figure 1). One of Xe^{131} excited states has a half-life of 12 days which is called the isomeric level $h11/2$. A vacuum system was used, (See Figure 2), to milk out the Xe^{131m} from I^{131}. A 50 mc of I^{131} was put in the system and after 13 days some stable Xe was introduced. The I^{131} solution was kept frozen all the time by surrounding it with a mixture of alcohol and dry ice. Part 3 was also surrounded with a mixture of alcohol and dry ice so that it traps the iodine gas, in case there is escaping gas out of Part 1. After a series of unfreeze and freeze for Part 1 the Xe gas was frozen in Part 2. Nitrogen liquid was around Part 2 which freezes the Xe gas. Then Part 2 was sealed off.
2. The Xe gas was sealed inside the glass tube and sent to Argonne National Laboratory. There the isotope separator was used to separate the Xe^{131} from other impurities and shoot it into the source holder. The source holder was made

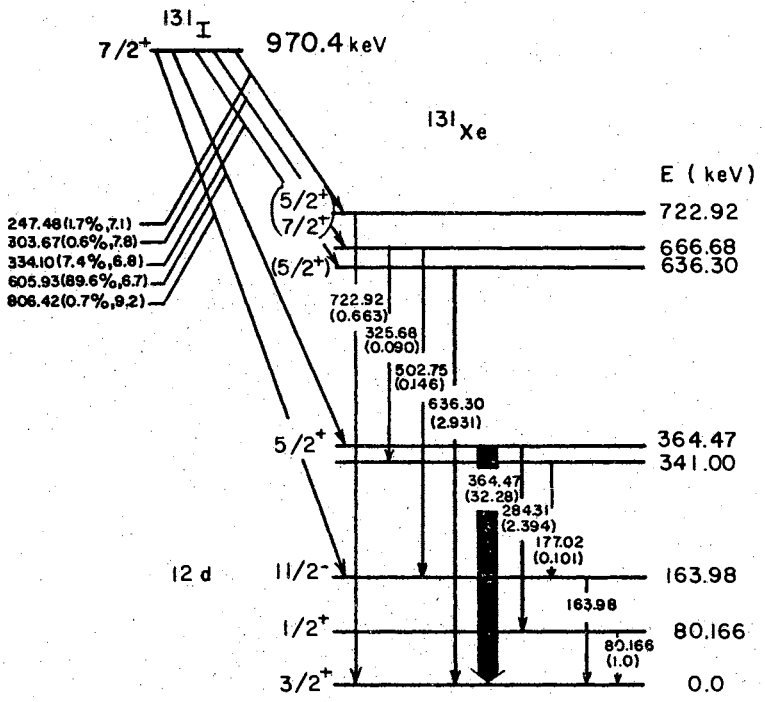

Figure 1. Energy Levels of Xe^{131} after the Decay of I^{131}

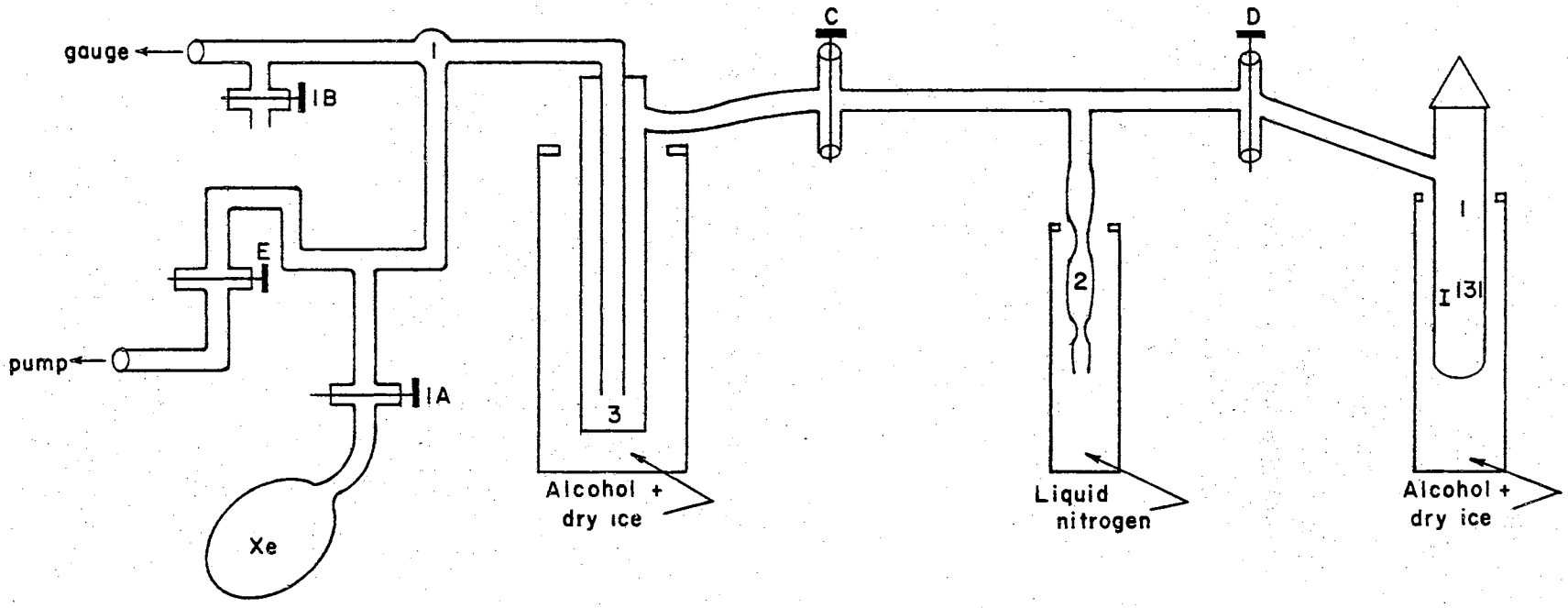

Figure 2. Vacuum System Assembly to Separate Xe^{131m} from I^{131}

of an aluminum foil of 3.5 mg/cm^2 which was glued on an aluminum ring of 19.9 mm diameter.

Experimental Arrangement

During the course of this work a number of different arrangements were used depending on the purpose of the measurement to be taken. The main arrangements only will be considered here. Other minor arrangements are not crucial to the experiment under discussion. Those major experiments are:

1. Investigation of intermediate level in the Xe^{131m} decaying to the ground state: In this case the Ge(li) detector was inside the source holder while the NaI detector was about 2½" from the source. Antiscattering shield, made of copper and lead, was used to prevent the back-scattering from one crystal to the other. A coincidence measurement was performed by sitting on the whole X-ray peak, with a window of 40 kev, in the NaI channel and accepting the whole spectrum in the Ge(li) channel.

   The NaI channel or the gating channel consists of the following:

   a. NaI(Li) crystal with 2" diameter and 0.04" thickness. This was integral line mounted on a RCA6342A photo-multiplier tube.

   b. Preamplifier Stump Model 1405

      This preamplifier is a charge sensitive device which integrates the output signals from the detector. Its stability is better than 0.01% per C^o and its integral non-linearity is less than 0.2% for 0 to ± 1.3 volts into 100

ohms. It contains an operational type amplifier, whose feedback from output to input is through a capacitor. The voltage developed across this capacitor is proportional to the charge from the detector. The operational amplifier is followed by a white emitter follower, which was designed to drive low impedance lines terminated in their characteristic impedance.

c. Linear Amplifier Model 1410 (Canbara Industries Inc.).

The Model 1410 linear amplifier provides in one module energy pulse shaping mode presently utilized for high resolution nuclear spectroscopy and counting. Through convenient front panel selection, one could be able to switch this amplifier into single or double differentiated delay line or RC shaping modes.

In the RC pulse shaping mode, RC time constants are switch selectable from 0.1 to 7 microseconds. In the delay line mode, there is a 1.2 microsecond delay line. Four prompt and delayed unipolar and bipolar outputs are simultaneously available from the front panel. This allows use of the single differentiated signal for energy resolution while the double differentiated signal is used for zero crossing timing purposes. The delayed signals are then available for multichannel pulse height analysis. There is a unique feature of this amplifier that is that there is an internal switch which removes integration from the bipolar outputs in order to obtain the sharpest zero crossing timing while retaining integration on the unipolar signals for

optimum energy analysis in the multichannel analyzer. The unipolar output was taken to the single channel analyzer and the bipolar output was fed into the zero strobe. The amplifier was in double delay lines mode.

d. Zero Strobe Model 1420

It was used to detect the zero crossing point of double delay line shaped pulses for precise timing of the incidence of these pulses in the detector. It generates a timing signal when the output signal of a double differentiating linear amplifier crosses the zero voltage baseline. This timing signal is then used by a fast coincidence unit for time coincidence evaluation of two more pulses.

The advantage of using this timing identification is that there will be a minimal timing signal shift due to amplitude variations in the output signal from the linear amplifier. The total timing shift due to signal amplitude in the sturup zero strobe is less than 1 nanosecond over a range of 0.5-8.0 volts. The stability of the delay setting is better than $\pm$ 0.3 nanoseconds per C^{o} from 25 to $50C^{o}$. The internal discriminator linearity is better than 1% (integral) of full range, 0.3 to 10.0 volts. The output of the strobe was fed into the fast coincidence unit.

e. Single Channel Analyzer Model 1430 (Canbara)

This single channel analyzer is used to sort, from all input pulses, those that fall within a pre-selected energy range. It generates an output (or logic) pulse whenever the input signal pulse from a pulse shaping amplifier falls

between two chosen voltage or energy levels determined by separate baseline and window width controls. Or, if selected to operate in the discriminator made, the unit operates as a simple baseline discriminator, generating an output pulse, whenever the input signal is above the lower level or baseline setting.

By means of an external strobing feature, an external strobing pulse allows the output of the single channel analyzer to be synchronized with the fast coincidence module output so that both signals can be applied to a slow coincidence module for concurrent time and energy analysis without further delay adjustments. This single channel analyzer was used in this experiment to select the window on the X-ray peak which is to be in coincidence with the whole spectrum in the Ge(li) channel. The output of it was fed into the fast coincidence unit.

The Ge(li) channel consists of the following:

a. Ge(li) Detector

It is a Coaxial Lithium Drifted Germanium detector. Its size is 2.56 mm diameter x 10.5 mm length. Drift depth is 7 mm, diffusion depth is 0.7 mm and its total active volume is 4.0 cc. Window to detector distance is 10 mm. There are absorbing layers of AL and Teflon with a thickness of 0.5 mm and 1 mm respectively. In this detector the germanium dead layer is zero. It has a resolution 2.8 kev Fwhm 1.33 mev at (-1000) volts bais and 2 microsecond. The drifted, or sensitive region, extends from the surface toward the center

of the device. Both the sensitive region and the P-type core are symmetric with the circumference along the entire length of the detector. This geometry assures uniform collecting fields and fast uniform pulse rise time characteristic of palaner devices while also providing the greater volume necessary for increased gama efficiency.

b. Tenelec Model TC130 preamplifier

It is a FET preamplifier specifically designed for use with cooled Lithium-drifted Germanium detector. Also it can be used, with minor or no modification, with any other kind of radiation detector such as silicon surface-barrier detectors, gridionization chambers, proportional counters and scintilation detectors. Its extremely low-noise characteristics make it particularly useful in high resolution Gamma-ray spectrometry. The lowest noise field-effect transistors commercially available are used in the input stage. It can be operated in any position and under practically all normal laboratory conditions. But is is not advisable to operate it at high temperature (above 50 or 60 C^{o}). Also it is very sensitive to strong vibration and ambicut noise which may have some deleterious effects on its performance. During the course of the experiment the whole system was shielded against the interference from outside noise. The output of the pre-amplifier was fed into the main pulse shaping amplifier.

c. Linear amplifier Model 1410 (Canbara)

As it was described in the NaI channel. The prompt bipolar output was fed into the zero-strobe and the prompt

unipolar output was fed into the delay amplifier.

d. Zero Strobe Model 1420

This was described in the NaI channel. During the course of the experiment the variable delay of the strobe was set on the position where the coincidence countrate is optimum. That was done by measuring the coincidence countrate as a function of the delay.

e. Delay Amplifier (Ortec Model 427)

This delay amplifier has a nominal gain of unity and provides the capability of linearly delaying a linear or logic signal from zero to 4.76 microseconds in 0.25 microsecond increments. The amount of delay is selected by five front panel switches. These delay lines are terminated in their characteristic impedance at both ends to minimize impedance mismatch and resultant pulse reflections on the lines. In this experiment a delay of 0.5 microsecond was used. The output of the delay amplifier was fed into the input of the multichannel analyzer.

The outputs of the zero strobes of the two channels were fed into the fast coincidence unit. The fast output of the fast coincidence unit and the output of the single channel channel analyzer in the NaI channel were fed into the slow coincidence unit. The output of the slow coincidence unit was used as gating pulse to the multichannel analyzer.

Fast Coincidence Unit Model 1440 (Canbara)

This unit is used to determine whether pulses occur within a

preselected time period of one another. It generates a logic signal output when the output pulses from 2, 3, or 4 zero strobes (or comparable zero crossing discriminators) all occur within the resolving time as set by front panel control. It has four channels A, B, C and D. To achieve a coincidence efficiency of one, channels A and B were modified to obtain maximum resolving time of the amount (175.9 $\pm$ 0.9) nanoseconds. This was measured very carefully using both two-source method and delay method. This value was obtained with a confidence level of 98%. The experiment was run with this resolving time.

Slow Coincidence Unit Model 1445 (Canbara)

The Model 1445 slow coincidence module generates simultaneous positive and negative routing or gating pulses whenever selected energy or energy and timing conditions are met simultaneously by the signals detected by two, three, or four detectors.

In the "slow" or energy analysis mode two or more signals are required to generate an output logic signal. In the "fast/slow" mode both the energy analysis conditions as preselected on the unit and a timing input pulse (typically from a fast coincidence unit) must be present. An "anticoincidence" input feature disables the unit when an anti-coincidence pulse is present. It is quite stable in the temperature range of 20^{o} to $55C^{o}$.

Multichannel analyzer (Nuclear Data, Inc. series 2200)

It is a completely modular multichannel analyzer in which the modules themselves are AEC compatible and may be placed in and operated from a standard AEC bin and power supply. The versatility of this

system is exemplified in that the analog to digital converter, master control, read-in/out display, and system memory. It can be constructed in sizes of 512, 1024, 2048, and 4096 channels. It has so many features that one cannot simply mention them here.

The data was read out with the Monroe Data/Log printer. The Omingraphic Recorder Model 6550 was used for plotting the spectrum.

Figure 3 shows the block diagram of the setup.

2. Search for the Double Quantum Emission Effect

In this experiment use was made of Ge(li)-NaI and Ge(li)-Si(li) detectors. The reason for using Ge(li)-Si(li) was to investigate the effect of the I escape peak in the case of the Ge(li)-NaI setup.

In the Ge(li)-NaI coincidence experiment the arrangement was the same as in Figure 3 except that the NaI detector now is in the source holder. But in the case of the Ge(li)-Si(li) coincidence experiment there were two arrangements. The first one was to look for the effect of I escape peak in which the Ge(li) channel was set on the 164 kev peak to gate the multichannel analyzer. The output of the slow coincidence was fed to a delay amplifier to match the internal delay in the multichannel analyzer. In the Si(li) channel the amplifier was 1417. The block diagram of this setup is in Figure 4.

The second one was to search for the double quantum effect as it was done with the Ge(li)-NaI. The experimental setup was the same as in Figure 4 except that the two detectors exchanged their positions. The window in the Si(li) channel was set on the X-ray peak to gate the multichannel analyzer. In both cases there was a 107 mg/cm^2 of AL between the Si(li) detector and the source which prevent the electrons

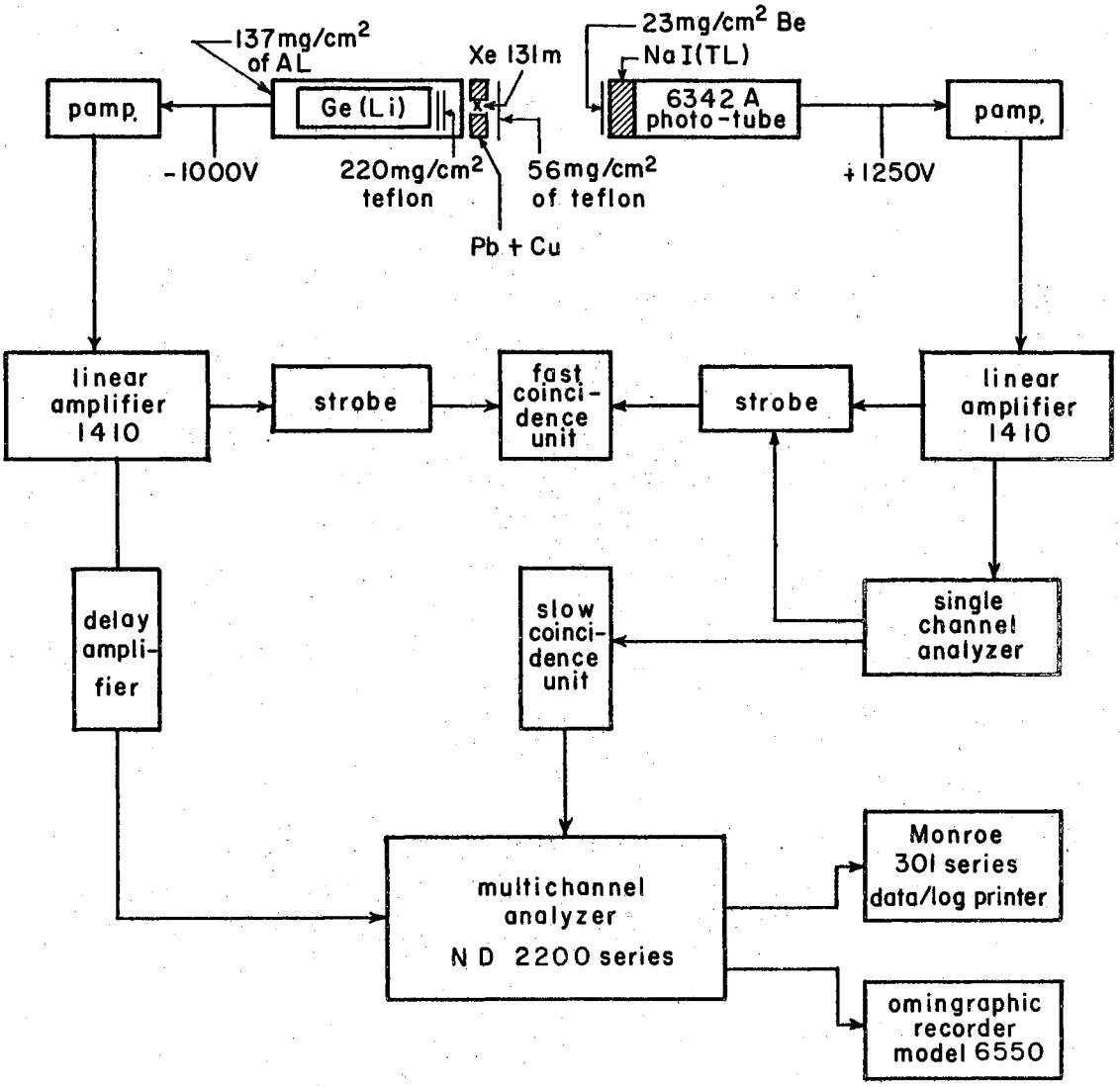

Figure 3. Block Diagram of the Ge(li)-NaI Coincidence Setup

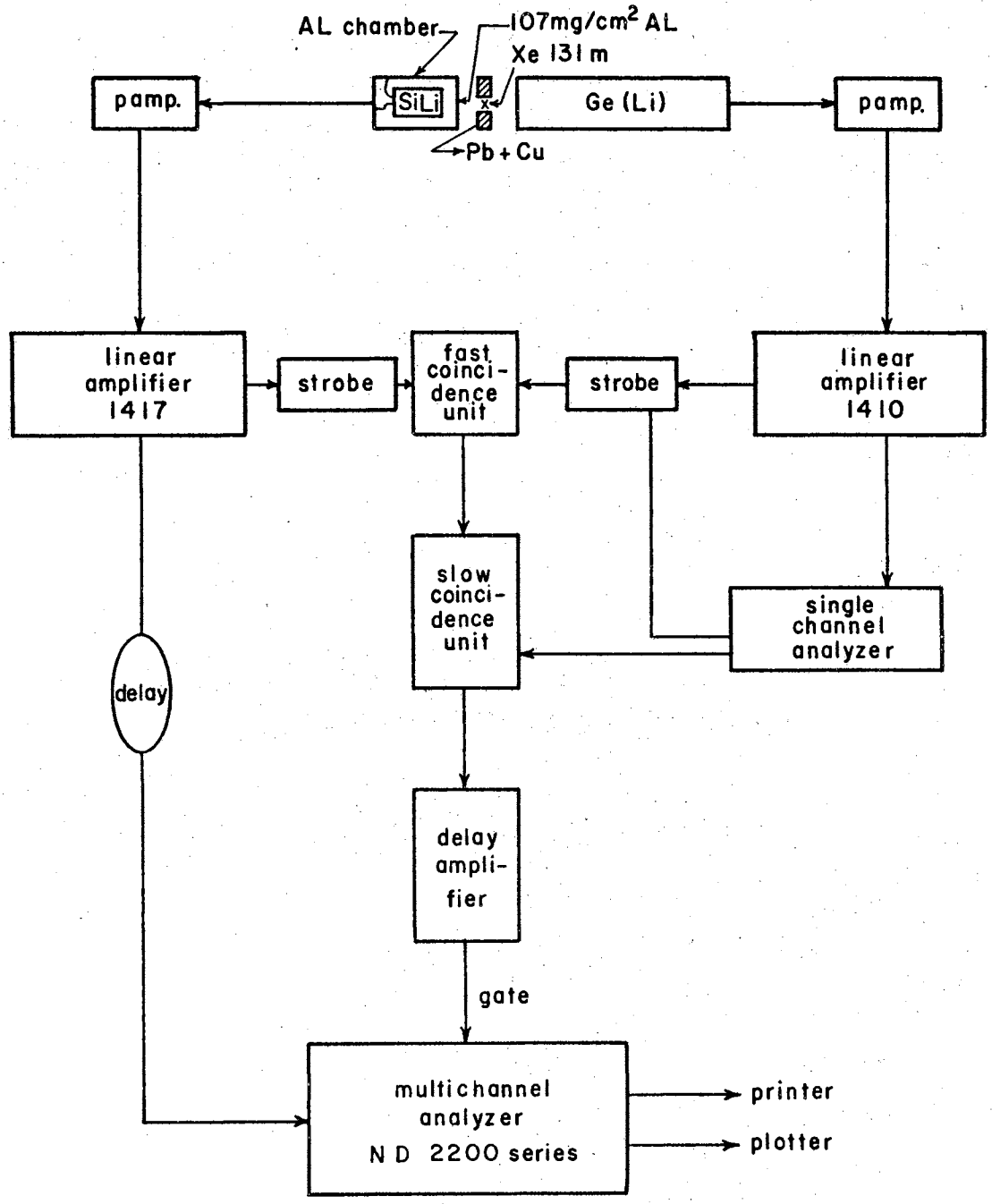

Figure 4. Block Diagram of the Ge(li)-Si(li) Coincidence Setup

from entering the Si(li) detector. This will be shown in the results.

3. Xe^{131} Spectrum with the Si(li) Detector

The aim of this experiment was to look for any possible conversion lines other than the 164 kev conversion lines. Also, it was used to demonstrate the effect of the absorber on the electrons. The silicon detector was enclosed in an aluminum chamber and kept under vacuum during the course of the experiment. Also, the detector was kept cool with the aid of a mixture of alcohol and dry ice. A liquid N_2 sorption pump provided a vacuum of better than 1 μ. The same preamplifier used with the Ge(li) detector was used with the silicon detector. In this experiment the source was inside the vacuum chamber. Spectra were also taken with the source outside, a case in which the K and L conversion lines disappeared indicating that the electrons did not penetrate the chamber window which is 107 mg/cm^2 of aluminum.

4. Si(li)-NaI Coincidence Experiment

This experiment was done to see whether there are coincidences between the continuum, which was observed in experiment 2, and the conversion electrons. The setup arrangement in this case is the same as in Figure 4 except that the NaI detector replaced the Ge(li) detector. The spectrum was looked at in the silicon detector while the window in the NaI channel was moved beyond the X-ray peak. The source was inside the aluminum chamber in front of the silicon detector. Under this arrangement no electrons are expected to go to the NaI detector because of the 107 mg/cm^2 aluminum window of the silicon detector chamber.

Collection of Data

For the coincidence experiment the system was tested with I^{125} which emits two coincidence X-rays of about 27.4 kev. Data was sorted in a multichannel analyzer.

In this type of experiment when one is searching for a very weak effect, it is necessary that experimental factors be optimized in so far as the experimental performance is not affected. For this reason a study of the coincidence countrate as a function of the delay was made and the result is shown in Figure 5. Also, study of the coincidence countrate as a function of the resolving time was made to establish the coincidence efficiency. It was found that the resolving time of the fast coincidence unit had to be increased to 180 nanoseconds in order to achieve a 100% coincidence efficiency.

The resolving time was measured by two methods, the two-source method and the delay method. In both cases use was made of the formula $N_{ch} = 2\tau N_1 N_2$, where N_{ch} = accidental coincidence counts, N_1, N_2 are the single counts and 2τ is the resolving time. It was measured at least twenty-five times and its value was established to be $2\tau = 175.9 \pm 0.9$ nanoseconds. This measurement has the confidence level of $\geq 98\%$.

The experiment was run under this resolving time which is corresponding to a 100% coincidence efficiency as is demonstrated in Figure 6.

The background was measured many times during the performance of the experiments and it was found negligible in the coincidence experiment but not so in the single spectrum. Since in our calculation use of the Nc(X) to the Nc(164) ratio was made, as also the ratio of Ns(X) to the Ns(164), a correction to the background was made for both the

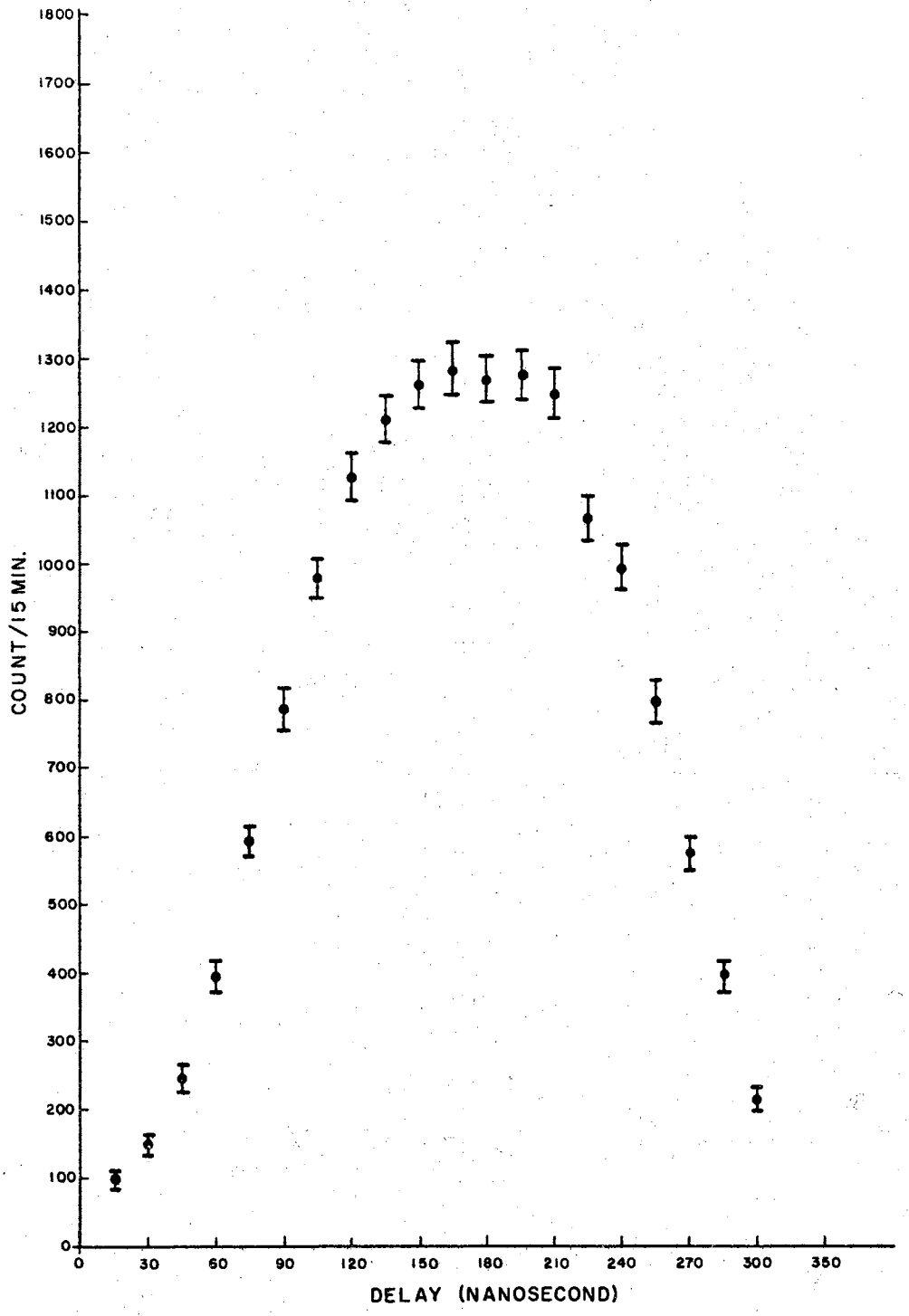

Figure 5. Coincidence Countrates as a Function of the Delay

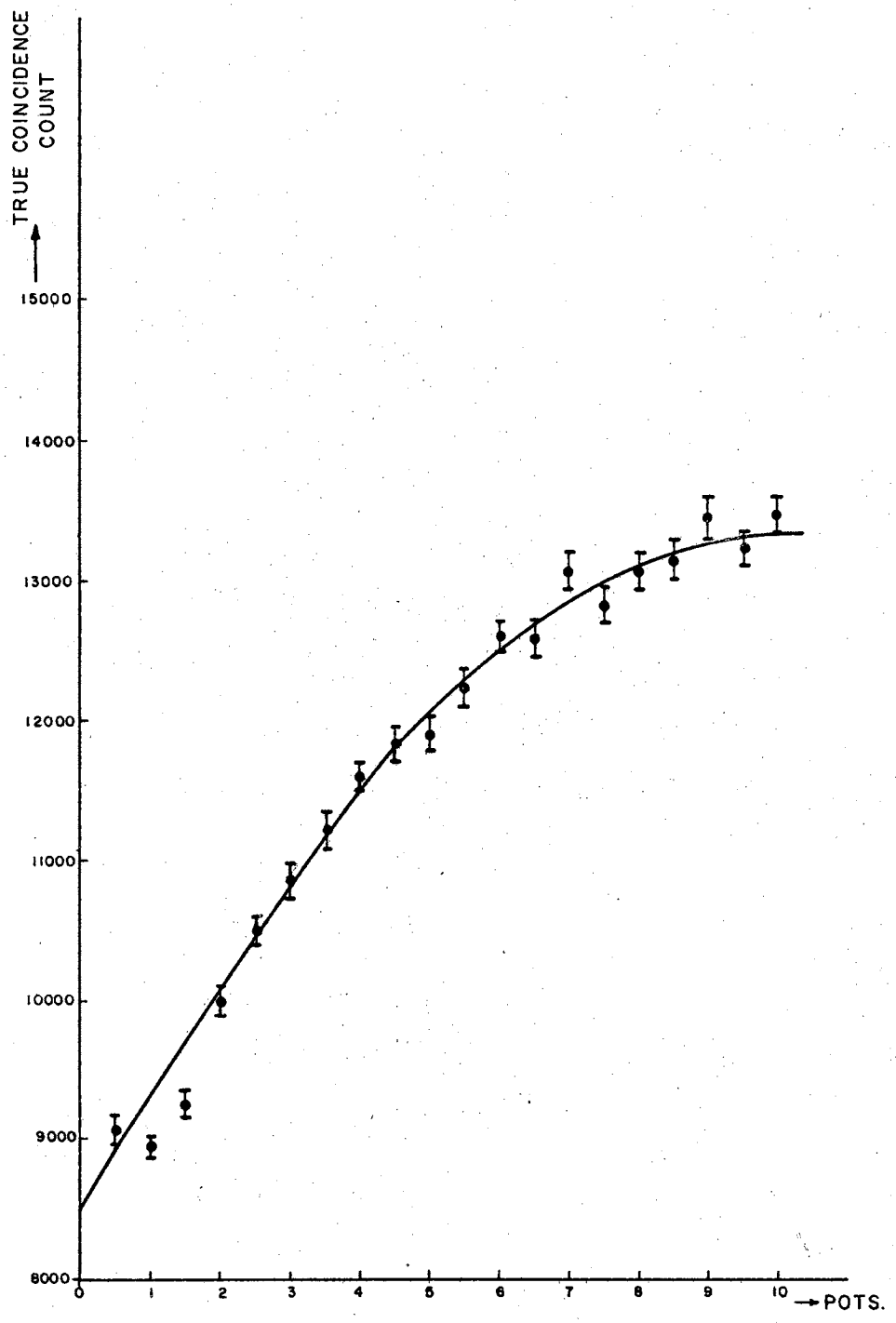

Figure 6. Coincidence Countrates as a Function of the Resolving Time.

coincidence and the single spectra. Nc(x) is the coincidence countrate in the X-ray peak and Nc(164) is the coincidence countrate in the 164 kev gamma-ray peak which are, in fact chance coincidences. Ns(x) and Ns(164) are the singles countrate of the X-ray peak and the gamma-ray peak respectively. It was experimentally shown that the ratio between Nx(x) and Ns(164) is the same as it is in the chance coincidence spectrum which gives another proof that the 164 kev peak in the coincidence spectrum is due to chance coincidences.

As another test for the electronic system the chance coincidence countrate in the 164 kev peak was calculated from the formula $N_{ch} = 2\tau N_1 N_2$ making use of the γ-ray peak single countrate and the single countrate of the NaI detector. It was found that in both cases the chance coincidence countrate is in good agreement which indicates that the electronic setup is functioning in the right way.

The Xe^{131m} was calibrated with the use of 3" x 3" NaI crystal. This type crystal was studied in detail by several authors[16,17] and its efficiency is very well established. It was found that the initial source strength is 1.3 μci.

During the course of the coincidence experiments the gating window was chosen with the aid of the multichannel analyzer.

Since there are many processes that could compete with the double quantum effect a number of test experiments were performed to study the possible effect of these other processes. All these will be discussed in detail in Chapter IV.

CHAPTER IV

DATA REDUCTION AND PRESENTATION

Analysis of Data

The coincidence spectrum which is shown in Figure (7) is due to the coincidence between events detected in the NaI(TL) crystal, which pass the energy selection of the single channel window, and those photons which go into the germanium detector. The observed coincidence countrate can then be expressed as:

$$N_{cx} = N_{xx} + N_{xh\upsilon} + N_{ch} \tag{1}$$

where $N_{xx} = N_o \Sigma_1(x) \Sigma_2(x) (2W_k^2 P_{xx} f' + \frac{\alpha_k \omega_k}{(1+\alpha)} P_{xhv} f)$

Here P_{xx} is due to the two coincident X-rays and $P_{xh\upsilon}$ is due to coincidence between X-rays and photons with energy such that it falls within the window. $N_{xh\upsilon}$ is due to photons going into the germanium detector and X-rays going into the window of NaI detector. The source of these photons could be due to either bremsstrahlung with the conversion electrons, or internal Compton effect or due to both of these effects. N_{ch} is the chance coincidence which can be expressed as

$$N_{ch}(X) = 2\tau N_o^2 E_1(X) E_2(X) W_k^2 (\frac{\alpha k}{1+\alpha})^2 \tag{2}$$

where 2τ is the resolving time of the coincidence circuit unit

N_o is the source activity

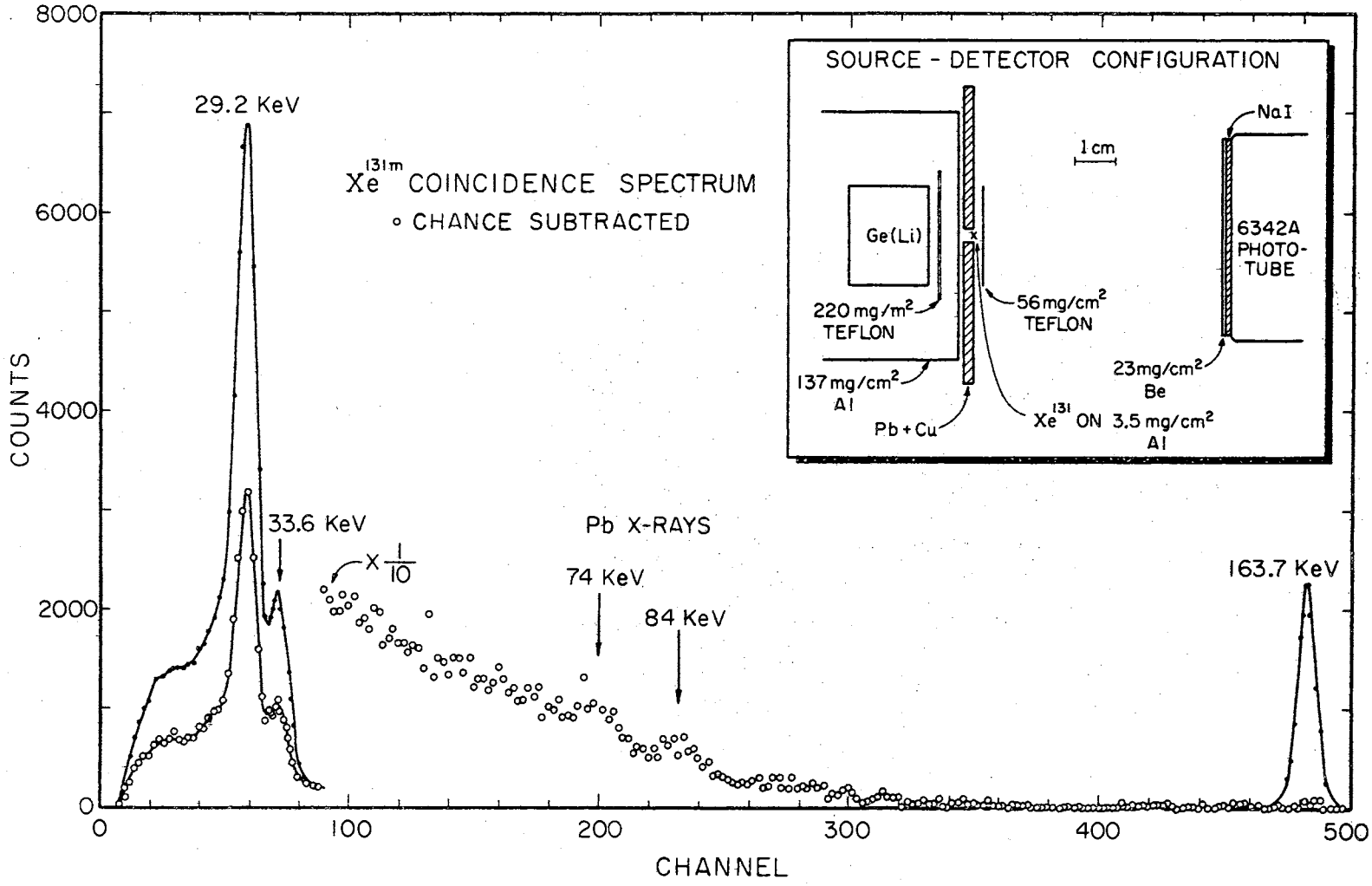

Figure 7. Coincidence Spectrum of Xe^{131m}

$E_1(X)$ is the Ge(li) detector efficiency

$E_2(X)$ is the NaI(TL) detector efficiency

W_k is the flourescence yield

α_k is the K-conversion coefficient

α is the total internal conversion coefficient

f' is the fraction of the X-ray peak in the NaI window with respect to the total peak.

f is the fraction of the photon continuum which might be included in the NaI(TL) window and it can be expressed as $f = \frac{N_{xh\upsilon}(xw)}{N_{xh\upsilon}(\gamma T)}$, where $N_{xh\upsilon}(xw)$, as defined before, is a part of the continuum which falls within the NaI window and $N_{xh\upsilon}(\gamma T)$ is the total of counts of the continuum. The coincidence countrates of the continuum in the Ge(li) detector can be expressed as

$$N_{xh\upsilon}(c) = N_o \Sigma_1(X)\, \Sigma_2(X)\, \left(\frac{\alpha k W_k}{1+\alpha}\right) P_{xh\upsilon} f \tag{3}$$

From equations (1) and (3) one finds that

$$N_{cx} - N_c(\text{Cont.}) = N_{xx} + N_{ch}(X) = N^c_{xx} \tag{4}$$

$$\text{If } n_{xx} = \sum_{F_1}^{F_2} N^c_{xx} = F\, N^c_{xx} \tag{4'}$$

where F_1 is lower limit of the sum on the peak and F_2 is the upper limit, then n_{xx} can be expressed as

$$n_{xx} = F\, N_o\, \Sigma_1(x)\Sigma_2(x)\left[2 P_{xx} W_k^2\, f' + \left(\frac{\alpha k}{1+\alpha}\right) W_k\, P_{xh\upsilon} f\right] +$$

$$F\, 2\tau\, N_o^2 \Sigma_1(x)\Sigma_2(\;)\, W_k^2\, \left(\frac{\alpha\, k}{1+\alpha}\right) f'$$

It was shown experimentally that $N_c(164) = N_\gamma$ is due to chance

and it can be expressed as:

$$N_\gamma = 2\tau\, N_o^2 \Sigma_1(x)\Sigma_2(X)\, \left(\frac{\alpha k}{1+\alpha}\right)^2 \frac{W_k}{\alpha_k}\, f' \tag{6}$$

where $E_1(\gamma)$ is the Ge(Li) detector efficiency for 164 kev gamma. The single countrates of the X-ray and the gamma ray can be expressed respectively as:

$$\begin{aligned} N_{sx} &= N_o\, \Sigma_1(X)\, W_k\, \left(\frac{\alpha k}{1+\alpha}\right) \\ N_{s\gamma} &= N_o\, \Sigma_1(\gamma)\, \left(\frac{1}{1+\alpha}\right) \end{aligned} \tag{6}$$

Taking the same fraction F for the same limits as in the coincidence case one can write that:

$$\begin{aligned} n_{sx} &= F\, N_o\, \Sigma_1(X)\, W_k\, \left(\frac{\alpha k}{1+\alpha}\right) \\ n_{s\gamma} &= N_o\, \Sigma_1(\gamma)\, \frac{1}{(1+\alpha)} \end{aligned} \tag{7}$$

From equation (7) one gets the relationship:

$$\frac{\Sigma_1(X)}{\Sigma_1(\gamma)} = \frac{1}{F\alpha_k W_k} \cdot \frac{n_{sx}}{n_{s\gamma}} \tag{8}$$

From equations (5), (6) and (8) it follows that:

$$A(y) = P_{xx} + \Sigma(f_{/f'}) = \frac{1}{2}\, 2\tau\, N_o \left(\frac{\alpha k}{1+\alpha}\right)^2 \left[\frac{n_{xx}}{N_\gamma} \cdot \frac{n_s}{n_{sx}} - 1\right] \bar{e}^{\lambda t} \tag{9}$$

where Σ is defined as:

$$\Sigma = \frac{1}{2W_k} \left(\frac{\alpha k}{1+\alpha}\right) P_{xh\upsilon}$$

A(y) is the total measured effect. Other symbols are as defined earlier and y is a function of window width. $e^{-\lambda t}$ is the source decay correction. From equation (9) one can write:

$$\begin{aligned} P_{xx} &= A(y) \quad -\Sigma\cdot(f/f') \\ &= A(y) \quad -\sigma\cdot(R/f') \end{aligned} \tag{10}$$

σ , R will be explained later.

Calculation of A(y)

Since N_γ in equation (9) is the chance coincidence countrates in the 164 kev peak, this can be expressed as:

$$N_\gamma = 2\tau N_\gamma(w) \quad n_{s\gamma} \tag{11}$$

where $N_\gamma(w)$ is the single countrate in the NaI window, and $n_{s\gamma}$ is the single countrate in the 164 kev peak. Therefore A(y) can be expressed as:

$$A(y) = \frac{1}{2}\, 2\tau\, N_o \left(\frac{\alpha' k}{1+\alpha}\right)^2 \left[\frac{n_{xx}}{2\, N_\gamma(w) n_{sx}} - 1\right] e^{\lambda t} \tag{12}$$

In equation (12) above n_{xx} must be taken after the correction for the continuum. The correction for the continuum was made as follows. Under the assumption that the continuum is mostly due to bremsstrahlung, it is expected that the flux (energy times counts times a correction factor for the detector efficiency) falls on a straight line, when plotted against energy. This is found to be nearly satisfied and the straight line passing through the continuum points is extrapolated to the left side of the X-ray peak. Then flux points were taken at each channel and converted back to counts and subtracted point by point

from N_{cx} in the X-ray peak. Then one would be left only with N^c_{xx} from which n_{xx} can be deduced (see equation 4′).

Calculation of $(\Sigma \cdot f/f')$

In order to determine the value of this term an experiment was done where the NaI window was set beyond the X-ray peak with a width of about 40 kev. A coincidence was observed in the X-ray peak. Some of these coincidences are expected to be due to X-rays and photons in the continuum. The total coincidence countrates can be expressed as:

$$N_c = N_o \Sigma_1(X)\, \Sigma_2(\gamma)\, W_k \left(\frac{\alpha \cdot k}{1+\alpha}\right) P_{xh\nu} f_w + N_{ch} \qquad (13)$$

where $\Sigma_2(\gamma)$ is the NaI detector efficiency for energy between 50 kev and 100 kev. f_w is the fraction of the continuum in this particular window and can be expressed as: $f_w = \frac{N_{xh\nu}(\gamma\omega)}{N_{xh\nu}(\gamma T)}$, where $N_{xh\nu}(\gamma\omega)$ is the $N_{xh\nu}$ counts in the continuum window of NaI detector and $N_{xh\nu}(\gamma T)$ was defined earlier. From equation (13) one can write that:

$$N^c_{xh\nu} = N_o \Sigma_1(X)\, \Sigma_2(\gamma)\, W_k \left(\frac{\alpha k}{1+\alpha}\right) P_{xh\nu}\, f_w = N_c - N_{ch} \qquad (14)$$

From equation (14) and the X-ray single countrate (see eq. 6′) one finds that:

$$\frac{N^c_{xh\nu}}{N_{sx}} = \Sigma_2(\gamma)\, P_{xh\nu}\, f_w$$

from which it follows:

$$P_{xh\nu} f_w = \frac{1}{\Sigma_2(\gamma)} \cdot \frac{N^c_{cxh\nu}}{N_{sx}} \qquad (15)$$

$\Sigma(f_{/f'})$ can be written as:

$$\Sigma\cdot(f_{/f'}) = \frac{1}{2W_k}\left(\frac{\alpha k}{1+\alpha}\right) P_{xh\upsilon}\, f_w\, (f_{/f'})$$

$$= \frac{1}{2W_k}\left(\frac{\alpha k}{1+\alpha}\right)\cdot\frac{1}{\Sigma_2(\gamma)}\,\frac{N^c_{xh\upsilon}}{N_{sx}}\cdot\frac{1}{f_w}\cdot(f_{/f'})$$

$$= \sigma\cdot(R_{/f'})$$

where $\sigma = \frac{1}{2W_k}\left(\frac{\alpha k}{1+\alpha}\right)\cdot\frac{1}{\Sigma_2(\gamma)}\cdot\frac{N^c_{xh\upsilon}}{N_{sx}}$

and $R = (f_{/f_w})$. All other symbols are as defined before. From this particular experiment and its corresponding single run it was found that:

$$\frac{N^c_{xh\upsilon}}{N_{sx}} = (.304 \pm 0.015)\times 10^{-3}$$

$\Sigma_2(\gamma)$ was taken from reference[16] to be 0.46 ± 0.01

$\alpha_k = 29$

$\alpha = 41.6$

$W_k = 0.87$

Using these values one finds that:

$$\sigma \cong 0.26 \times 10^{-3}$$

Table II gives A(y), $(\sigma R_{/f'})$ values as functions of window.

The indicated errors are based on the estimate of possible instrumental errors as well as statistical uncertainties. Before coming to the discussion and evaluation of P_{xx} from Table II, one has to consider any other possible processes which might contribute to the coincidence countrates which contribute to A(y). The following effects were

TABLE II

A(y) AND $\sigma \cdot (R_{/f})$ WITH DIFFERENT WINDOW WIDTH

Window Width kev	$R_{/f}$	$\sigma \cdot R_{/f} \times 10^{-3}$	$A(y) \times 10^{-3}$
20	2.64 ± 0.3	0.59 ± 0.06	0.74 ± 0.04
14	1.99 ± 0.2	0.44 ± 0.05	0.58 ± 0.03
10	1.77 ± 0.18	0.4 ± 0.04	0.57 ± 0.03
8.3	1.76 ± 0.18	0.39 ± 0.04	0.87 ± 0.03
5.6	1.75 ± 0.18	0.39 ± 0.04	0.45 ± 0.03
4.4	1.58 ± 0.16	0.51 ± 0.04	0.51 ± 0.03
3.4	2.25 ± 0.2	0.51 ± 0.05	0.46 ± -.03
2.5	3.22 ± 0.3	0.72 ± 0.06	0.54 ± 0.03

considered:

1) impurities in the Xe^{131m} sample
2) chance coincidences
3) coincidences between K-conversion electrons and K X-rays
4) multiple scattering between the two detectors
5) K electron ionization of Xe by the emitted K conversion electron

6) external Compton effect

7) an intermediate level.

Other Possible Processes Which Might Contribute to the Coincidences

1. Impurities in the Xe^{131m} Sample

The sample was electromagnetically isotope separated at Argonne National Laboratory. Under these conditions, only activities with mass number 131 could occur, possible I^{131}. To look for this and other possible impurities a spectrum of Xe^{131} was taken for a reasonably long time. It was found that a Co^{57} impurity is less than 0.005% and other possible impurities are far less than 0.001%. This can give rise to true coincidences between gamma-rays and X-rays. The contribution to the observed coincidence countingrate from I^{131} has been investigated by making use of pure I^{131} source which was about 18 times stronger than the impurities of I^{131} in the Xe^{131} sample. With the use of the coincidence countingrate in the x-peak in Xe^{131} coincidence spectrum and that of pure I^{131} it was possible to estimate the coincidence countingrate due to the I^{131} impurities to be = 8 counts per 10 hours compared to 7700 counts per ten hours in the Xe^{141} x-peak. This gives about 0.1% contribution which is considered quite negligible. The other impurities' contribution is, therefore, also negligible.

2. Chance Coincidences

This was measured by introducing a delay of 700 nanosecond in the gating pulse side. Due to the fact that the source activity was about 1.3 μci and that the resolving time was at maximum value (175.9 $\pm$ 0.9 nanoseconds) the true to chance coincidence ratio varies from 2 to 6

depending on the time when the measurement was made. But since P_{xx} was calculated from equation (10) it was not necessary to subtract the chance coincidence counting rate. A comparison of the real and chance coincidence spectra is shown in Figure 7. The background coincidence counting rate was found to be negligible. By background one means that the source is not present.

3. Coincidences between K-conversion Electrons and KX-rays

It is quite possible that some K electrons penetrate into the X-ray crystal, which can give rise to real coincidences between the K electrons and KX-ray. In order to avoid this, a careful study was made to estimate the possible number of electrons which might penetrate into the crystal in spite of placing an absorber of more than 60 mg/cm^2 thickness, a thickness which exceeds twice the range of electrons with an energy of 130 kev. This was done with the aid of a silicon detector which has a resolution of about 10 kev for all practical purposes. Figure 8 shows the Xe^{131} spectrum where the K and L lines are very well resolved. Figure 9 represents the Xe^{131} spectrum with an absorber thickness of 28 mg/cm^2 between the detector and the source while Figure 10 represents the case when the absorber thickness was 56 mg/cm^2. Further, the source was taken outside the chamber of the silicon detector, the window of that chamber being about 107 mg/cm^2. The spectrum in this case is given in Figure 11. From Figure 10 and Figure 11 it was possible to estimate the ratio between the possible penetrating electrons and the initial electrons where no absorber was present. This was based on the assumption that in Figure 11, there is no possibility of the electrons penetrating through the 107 mg/cm^2

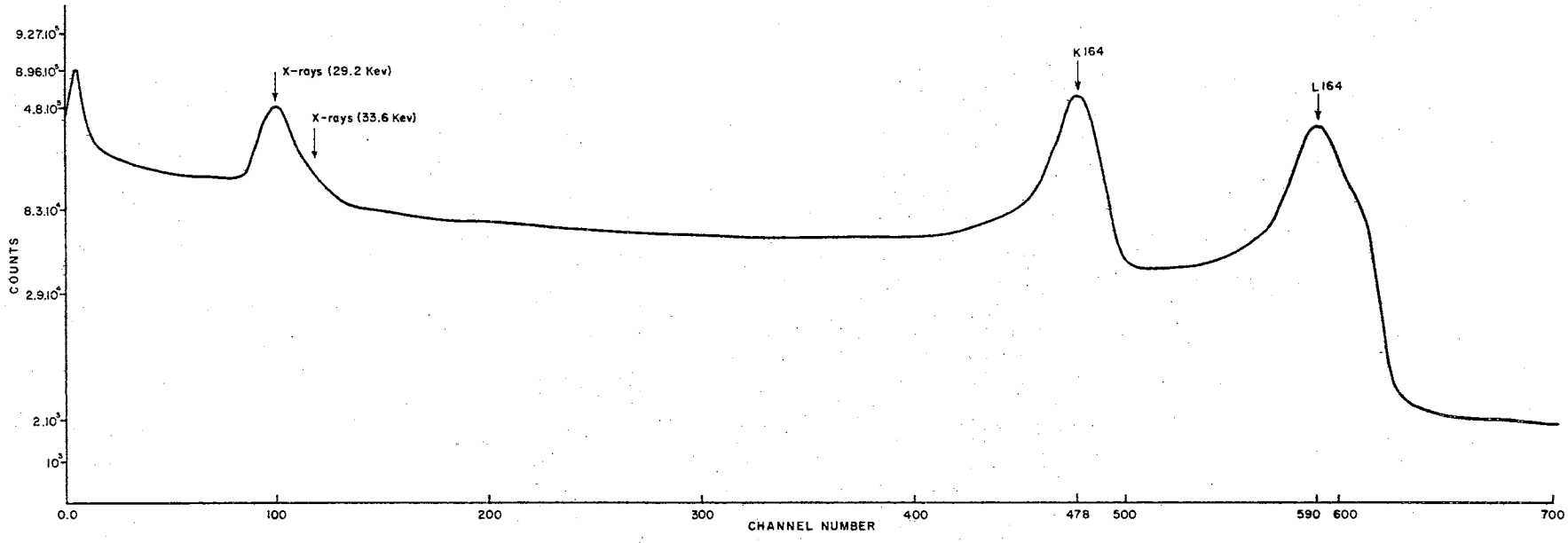

Figure 8. Xe^{131m} Single Spectrum Taken by the Silicon Detector

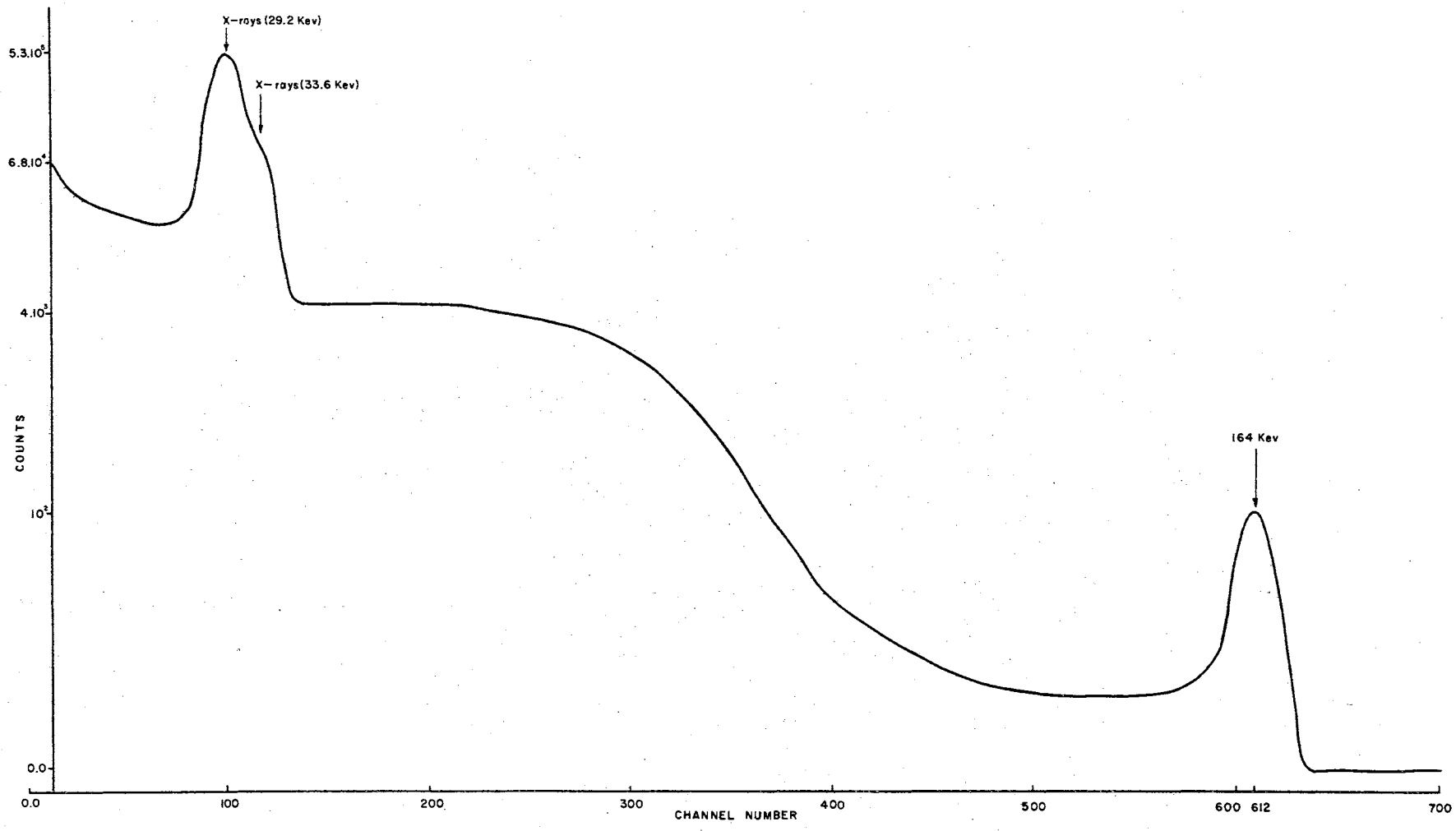

Figure 9. Xe^{131m} Single Spectrum Taken by the Silicon Detector with an Absorber Thickness of 28 mg/cm^2 between the Detector and the Source

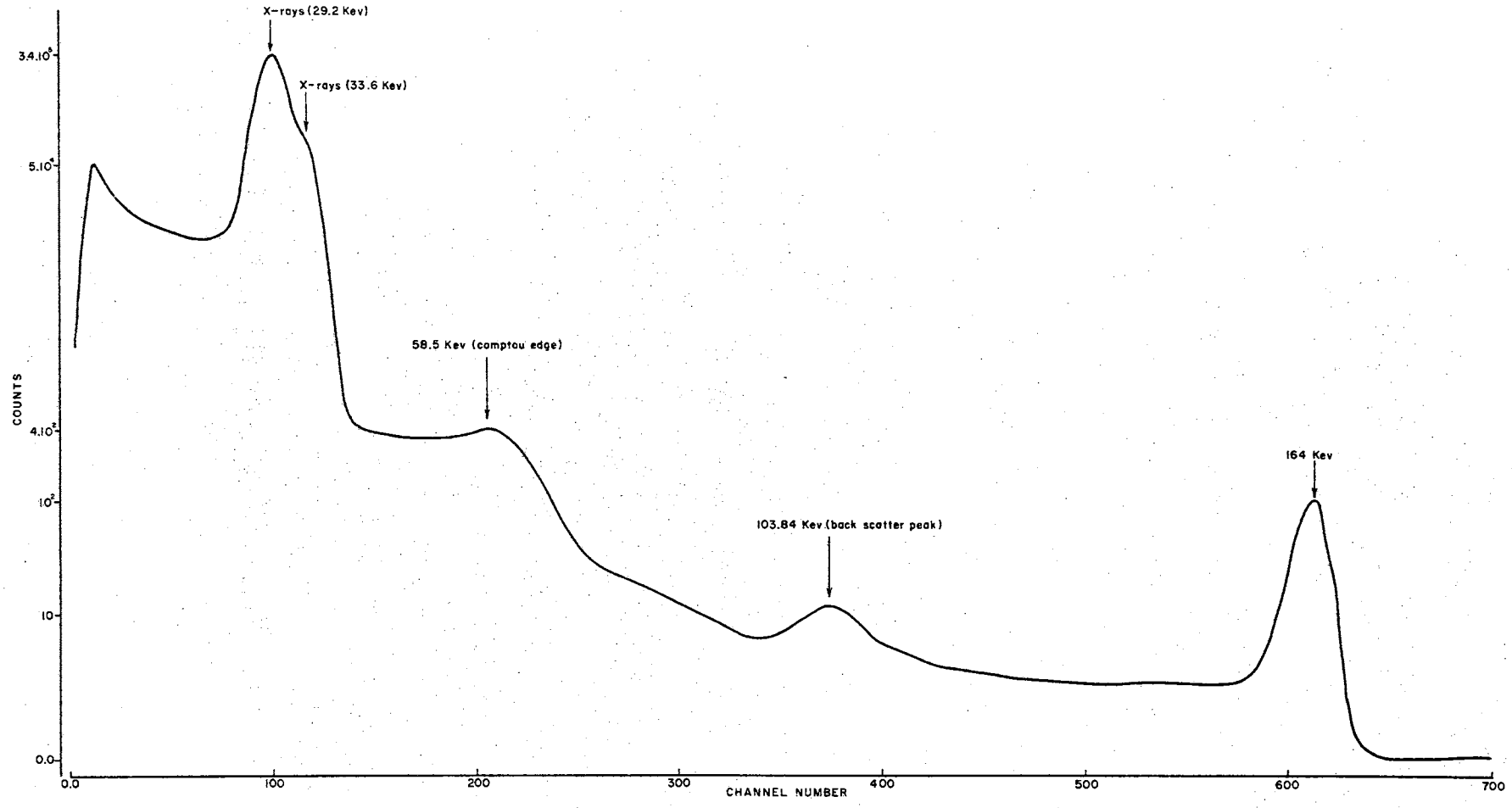

Figure 10. Xe^{131m} Single Spectrum Taken by the Silicon Detector with an Absorber Thickness of 56 mg/cm^2

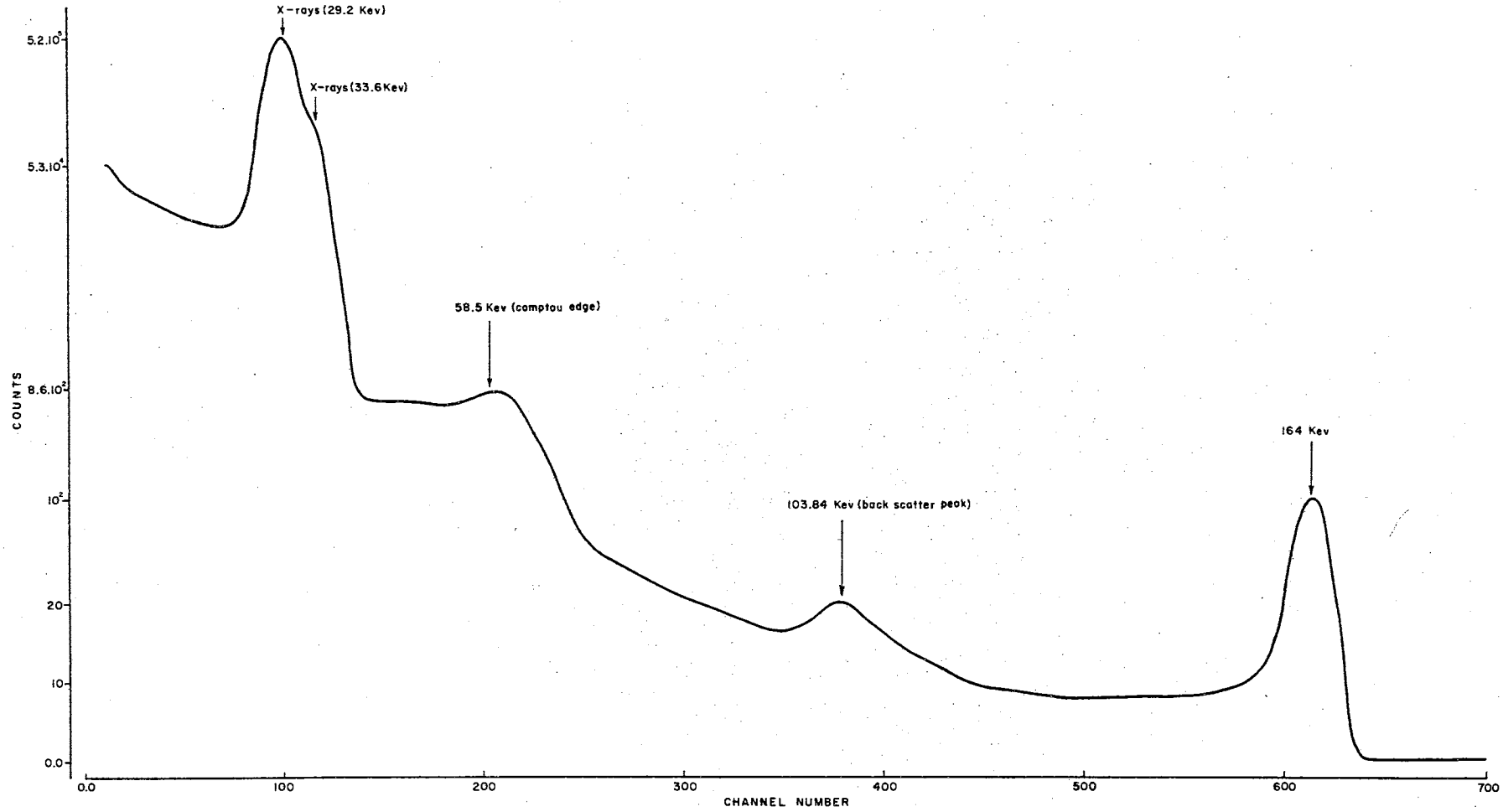

Figure 11. Xe^{131m} Single Spectrum Where the Source is Outside the Silicon Detector Chamber

absorber to the detector but a possibility of penetration through the 56 mg/cm^2 absorber. The counts in Figure 11 were subtracted from the counts in Figure 10 and the difference was considered as an upper limit to the number of electrons which might possibly penetrate into the X-ray crystal. It was found that the number of left electrons is about 10^{-4} of the initial number. Further, as the efficiency of NaI(TL) for electrons is only about 10%, one can estimate that the total possible contribution to the observed peak intensity from X-ray K electron coincidences is no more than 0.2%. This can be verified using the formula:

$$N_c(e_1x) = \left(\frac{\alpha k}{1+\alpha}\right) N_o \Sigma_1(e) \Sigma_2(x) W_k f(x) \qquad (16)$$

where

$N_c(e_1x)$ = coincidence counting rate between electrons and X-rays

$\Sigma_1(e)$ = efficiency of the NaI(TL) for the electrons

$f(x)$ = X-ray transmission factor which is approximately one.

The other symbols are similar to those used in equation (1).

$$W_K = 0.87 \text{ for } Xe^{131}$$

$$\Sigma_1(e)\Omega_1 = 0.045$$

$$\Sigma_2\Omega_2 = (15.6 \pm 3.9) \cdot 10^{-3}$$

$\Sigma_2\Omega_2$ was calculated from the relation:

$$N_s(x) = N_o \Sigma_2\Omega_2 \left(\frac{\alpha k}{1+\alpha}\right) W_K \qquad (17)$$

Where $N_s(x)$ is the total count under the X-ray peak in the single spectrum of Xe^{131}.

From equation (16) one finds that $N_c(e_1x)$ = 2 cps = 120 cpm if the whole K electrons penetrate into the X-ray crystal. But that was not the case because of the 60 mg/cm^2 absorber. The number of penetrating electrons was found to be about 10^{-4} as an upper limit which gives about 0.012 cpm which is 0.2% of the observed coincidences. Therefore, it is negligible.

4. Multiple scattering between the two detectors

Backscattering from one detector to the other can contribute to some extent to the coincidence counting rate. This effect was largely suppressed by use of the lead and copper absorbers between the detectors. Under this antiscattering arrangement one might consider the contribution from this effect to be quite negligible. There is, in addition, a possible contribution to the coincidence countingrate from the iodine escape X-ray. This was found evident in the experiment when the window in the single channel analyzer was set on the 164 kev gamma-peak. It is very well known that the 164 kev gamma-ray is in no coincidence with anything in the Xe^{131} spectrum and it was appearing in the coincidence spectrum as chance. This was proved from the fact that the 164 kev peak in both the coincidence and the chance spectra is the same. However, when the window was set on this peak, it was found that an X-ray peak in the coincidence spectrum is still there. After careful investigation the peak was found to be a 28.4 kev which is the X-ray of iodine. What happened was that, when the 164 kev gamma-ray entered the NaI(TL) crystal, it excited the iodine atom and an iodine X-ray was emitted. This was further investigated by use of silicon detector and Ge(1i) detector where no real coincidence was shown. However, it

was found that the contribution from iodine escape X-ray was negligible.

5. K electrons ionization of Xe by the emitted K conversion electrons

Due to the isotope separation procedure an amount of stable Xe in the sample is necessary to be used as carrier. This amount of stable Xe in the sample was less than 0.2 microgram. It is quite possible that K conversion electrons ionize the K electrons of the stable Xe and X-ray will be produced. Thus this can give rise to real coincidences between two X-rays. A test experiment was done to investigate this cause by use of 211 mg/cm^2 of Ba. The thickness of stable Xe in the sample was calculated to be 2.5 gm/cm^2. It was found that the ratio between $N_c(x)$ and $N_c(164)$ is increased by about 50%. Since $N_c(164)$ is a pure chance coincidence, as is evident from the experiment, the increase in the ratio can only be due to the enhancement in the real coincidences in the X-ray peak. Part of the increase in the real coincidences could be due to increased bremsstrahlung too. Comparing the amount of stable Xe in the sample with the amount of Ba which was used in the test experiment one finds that the Xe to Ba ratio is about 10^{-5}. In this test experiment one expects that the effect will be magnified at least by a factor of two thousand--not by only 50%. Thus the K ionization must be completely negligible.

6. External Compton effect

This effect can give a contribution to the continuous distribution. However, this was taken care of by the evaluation of $N_{xh\upsilon}$ as mentioned earlier.

7. An intermediate level

The photon may not go directly to the ground state but pass through another level with specific energy, spin and parity. This can be a very competing effect because of the fact that a real coincidence between two X-rays is quite possible in this case. This could be verified experimentally.

With the use of the silicon detector (see Figure 7) it was found that the intensity of a possible conversion line other than the K 164 kev and L 164 kev lines in the decay of Xe^{131m} is about $1.3 \cdot 10^{-4}$ as an upper limit. From the decay scheme of I^{131} [22] one might expect that a single particle level, the $5\frac{1}{2}$ level, is a possibility for an intermediate state which implies that the decay to the ground state must go via an E_5 transition from $h_{\frac{11}{2}}^-$ to $S_{\frac{1}{2}}+$. However, the transition probability of E_5 is quite small, both experimentally[11] and theoretically compared to the M4 transition probability. This makes the transition $h_{\frac{11}{2}}^- \rightarrow S_{\frac{1}{2}}+ \rightarrow d_{\frac{3}{2}}+$ is unfavorable.

Moreover, one could measure the expected contribution to the real coincidences from this possible effect. This can be done with the aid of the following formula:

$$N_c(KX) = N_o \, \Sigma_1 \, \Omega_1 \, \Sigma_2 \, \Omega_2 \, \left(\frac{\alpha \, k}{1+\alpha}\right)^2 W_k^2 \, I(KX) \qquad (18)$$

Where I(KX) is the upper limit of the intensity for any possible electron line. $\alpha k_{/L+M}$ for E_5 is reported[11] to be about 0.009 and α is about one for an energy of about 80 kev. From equation (18) it was found that the real coincidences from this effect are less than 0.06 counts per twenty hours compared to an average of 3600 counts per

twenty hours of the observed coincidences. All this information indicates that the intermediate level, if it exists, contributes very little and the observed effect cannot be due to it.

A search for the intermediate level was, however, carried out because in principle, one should be able to detect the intermediate level as a peak in the continuous distribution. Such a peak was not found, as is clear from Figure 7. A search for any other possible level other than the $h_{11/2}$ level in the decay of Xe^{131m} was done too. An upper limit of about $1.13 \cdot 10^{-4}$ was found for the intensity of any possible peak with respect to the 164 kev gamma-ray peak. This is another evidence showing that the existence of any intermediate level is quite improbable.

Evaluation of P_{xx}

From equation (10) and Table II the value of P_{xx} was calculated for each window. Then the average of P_{xx} for the different windows was taken as an upper limit because of the fact that P_{xx} should be independent of the window if the effect does exist. However, this work showed that the effect is quite sensitive to the window setting which implies that only an upper limit can be deduced. This upper limit is calculated to be:

$$P_{xx} \leq (7.5 \pm 1.5) \times 10^{-5}$$

P_{xx} represents the ratio of a second order transition to a single order one. Since the observed peak in the coincidence spectrum is an X-ray peak, it can be concluded that the two X-rays which were observed in coincidence could be due to $\gamma\gamma$, $e_k\, e_k$, or $\gamma\, e_k$ emission. According to reference[12] $\gamma\gamma$ are to be ruled out. The observed effect, therefore,

is due to the emission of two K-quanta and these double K-quanta result either from a double conversion in the K shell or from the internal conversion of the internal Compton effect. Thus the measured value of P_{xx} is equivalent to the ratio $\frac{W_{e_k e_k}}{W_{e_k} + W_\gamma}$ where $W_{e_k e_k}$ is the transition probability for the simultaneous emission of two K-electrons, W_{e_k} is the transition probability of a single e_k electron and W_γ is the single gamma transition probability. $W_e = \alpha W_\gamma$ where α is the total internal conversion coefficient which, as reported in reference[12], has a value 53.3. From the relation between W_e and W_γ and making use of the flourescence yield, which has a value of 0.87 for Xe^{131}, one finds that $\frac{W_{kk}}{W_\gamma}$ $(3.1 \pm 0.6) \times 10^{-3}$. This result is compared to $(2.7 \pm 0.7) \times 10^{-3}$ of reference[12] and 1.85×10^{-2} of reference[11]. Also $\frac{W_{e_k e_k}}{W_\gamma}$ was found to be $\leq (4.1 \pm 0.8) \times 10^{-3}$. It was reported in reference[12] that $\frac{W_{e_k e_k}}{W_{\gamma\gamma}}$ is > 260 for E2M2 and > 130 for E1M3 and M1E3. From this it was possible to deduce the following upper limits for $\frac{W_{\gamma\gamma}}{W_\gamma}$,

$$\frac{W_{\gamma\gamma}}{W_\gamma} \leq (1.6 \pm 0.3) \times 10^{-5} \text{ for E2M2}$$

$$\leq (3.2 \pm 0.6) \times 10^{-5} \text{ for E1M3 or M1E3}$$

whereas for the latter multipolarity Knauf et al.,[12] have reported a limit of 2.2×10^{-5}.

CHAPTER V

ANGULAR CORRELATION MEASUREMENTS IN Sb^{125} DECAY

Introduction

The basic phenomenon of angular correlations can be stated as follows: a nucleus decays from a first level A by emitting a radiation γ_1, in the direction (K_1) into the intermediate state B and from there, through the emission of γ_2 in the direction (K_2), into the final state (as in Figure 12). Now the question is what is the relative probability $W(\theta)d\omega$ that the radiation γ_2 is emitted at an angle θ with respect to the direction K_1 of the radiation γ_1, into the solid angle.

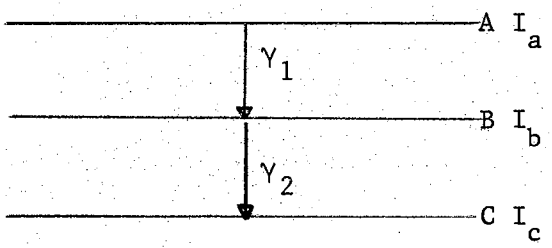

Figure 12. Radiations Emitted in Cascade

$W(\theta)$ has been calculated using perturbation theory[18] and shown to be

expressible as a series in Legendre polynomials

$$W(\theta) = 1 + A_2(1)A_2(2)P_2(\theta) + A_4(1)A_4(2)P_4(\theta) + ...$$

Decay Scheme of Sb^{125}

In order to make angular correlation measurements, one has to be sure that the decay of the nucleus, which is chosen for study, is very well established. The decay of Sb^{125} has been investigated by many authors[19,20,21] but the results have been somewhat conflicting regarding the spin assignment of the 0.321 Mev level in Te^{125}, which is the product of this decay. For example Narcisi[19] on the basis of the measured internal conversion coefficient of the 0.176 Mev transition assigns a spin of $9/2$ to this level. However, such a large spin is not predicted by the single particle model with a spherical nuclear potential. Glendenning[22] calculated the energy levels and the spins using the intermediate coupling model. This model shows that no assignment of $9/2$ spin could be predicted to levels other than the high levels at 0.931 Mev and 1.33 Mev. In addition to this controversy it has been reported[23] that there may exist a new 0.401 Mev level.

It was, therefore, felt necessary to re-measure the energy levels using high resolution detectors - the germanium solid state detectors, - so that one could be sure about the decay scheme before going into the angular correlation measurements. Moreover it is of importance to make sure that there are no impurities in the sample. The latter point can be confirmed by taking the singles spectrum of the isotope.

Experimental Technique and Methods

1. Single Spectrum of Sb^{125}

The source was deposited on an electric tape and kept in front of the germanium detector. The electronic assembly consisted of a pre-amplifier, amplifier and multichannel analyzer. All these components have been described in Chapter III. The system was calibrated using the standard sources Am^{241}, Co^{57} and Cs^{137}. The single spectrum is shown in Figure 13.

2. Assembly for the Angular Correlation Experiment

For this experiment two 2" x 2" NaI(TL) crystals were used. Each crystal was mounted on RCA 6342 photomultiplier tube. The apparatus consisted of two symmetrical channels, each channel consisting of a detector, a preamplifier and a single channel analyzer or pulse height selector. The output from each pulse height selector (differential) provided the input pulses to a coincidence circuit. The coincidence circuit was a replica of the Advance Radiation Engineering Corporation Model 401 coincidence-anticoincidence unit. It has three channel logic modes (triple coincidence circuit), and a resolving time which is adjustable from 0.5 to 20 microseconds. In this work, the coincidence circuit was adjusted to a resolving time of 1.4×10^{-6} sec as determined by performing an experiment with two independent sources with the detectors separated from each other by lead shielding. To calculate the resolving time the following formula was used:

$$N_{ch} = 2 \tau N_1 N_2$$

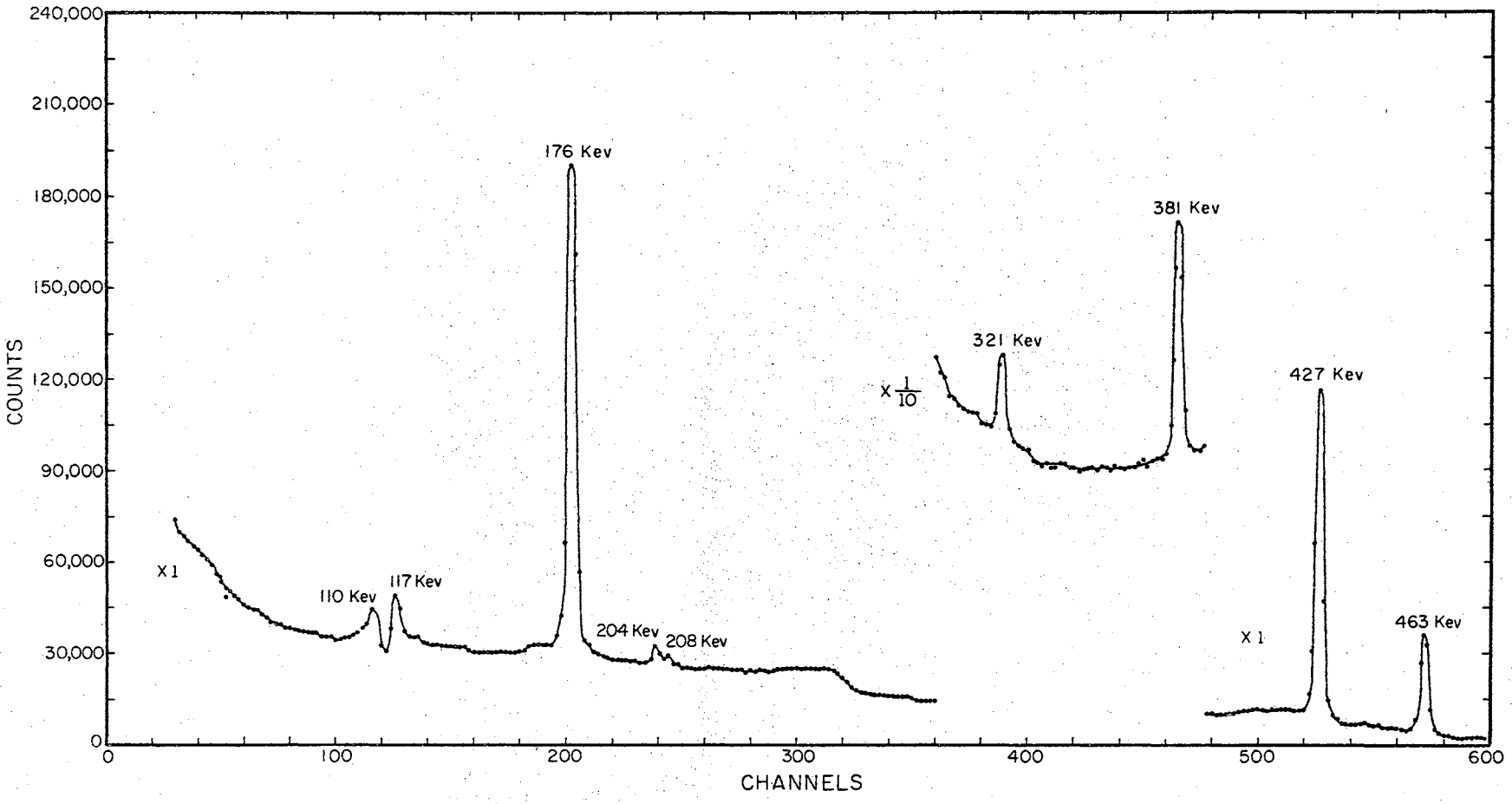

Figure 13. a) Single Spectrum of Sb^{125} in the Range 110 kev to 463 kev.

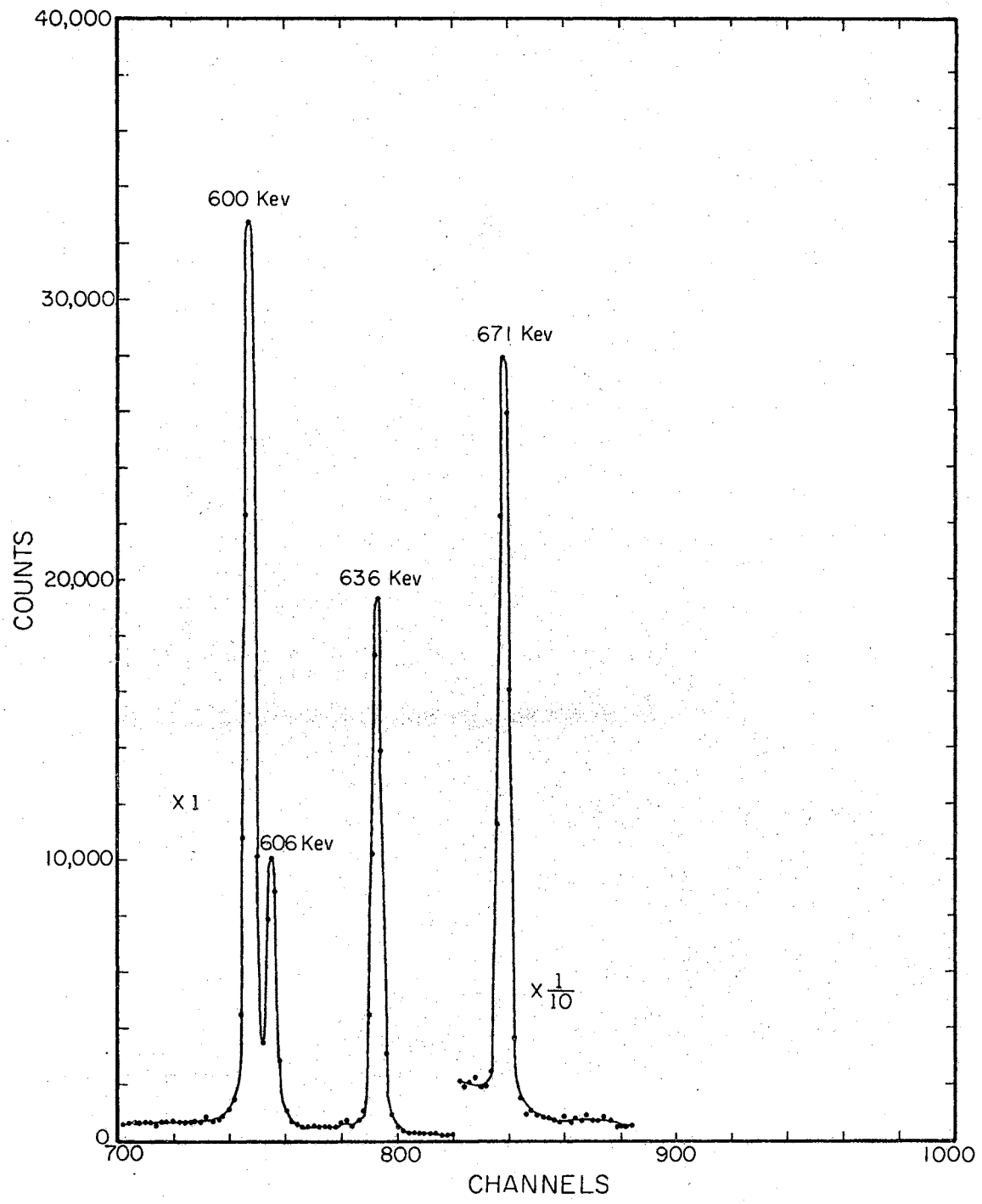

Figure 13. b) Single Spectrum of Sb^{125} in the Range 600 kev to 671 kev.

where N_{ch} is the chance coincidence, N_1, N_2 are the single counting rates and 2τ refers to the resolving time of the circuit. The block diagrom of this arrangement is shown in Figure 14.

In this case a special apparatus was designed which consisted of two arms attached to a 360^{o} scale plus a vernier scale. One of these arms was fixed and the other was movable along a circular path. The source was deposited on a mylar foil of 0.01 mm thickness and covered with an identical foil, forming a "sandwich" wrapped around a hollow lucite cylinder 3 mm in diameter. The lucite cylinder was fitted to stand on edge on an aluminum cylinder. The readings were taken at angles 90^{o}, 120^{o}, 150^{o}, and 180^{o}. A check was made to see if the arrangement was symmetrical by obtaining the readings at the angles 270^{o}, 240^{o}, 210^{o}. It was found symmetric within statistical errors. The energies of the two γ rays which are to be studied were selected with the aid of the single channel analyzer. Each ray was chosen carefully so that any possible interference from adjacent rays was negligible. This was done with the aid of the window of the single channel analyzer. The coincidence counts were registered with a TMC model SH-3A2 scaler equipped with a discriminator and a timer.

Determination of the Angular Correlation Coefficients

After the coincidence counts were corrected for chance coincidences, background, normalization of the product of the singles count rates was carried out. The normalization was done to take care of any possible shift in the singles count rates. Using the least squares method developed by Rose[24] the coefficients A_2 and A_4, which establish the angular correlation function for the two - cascade, were obtained.

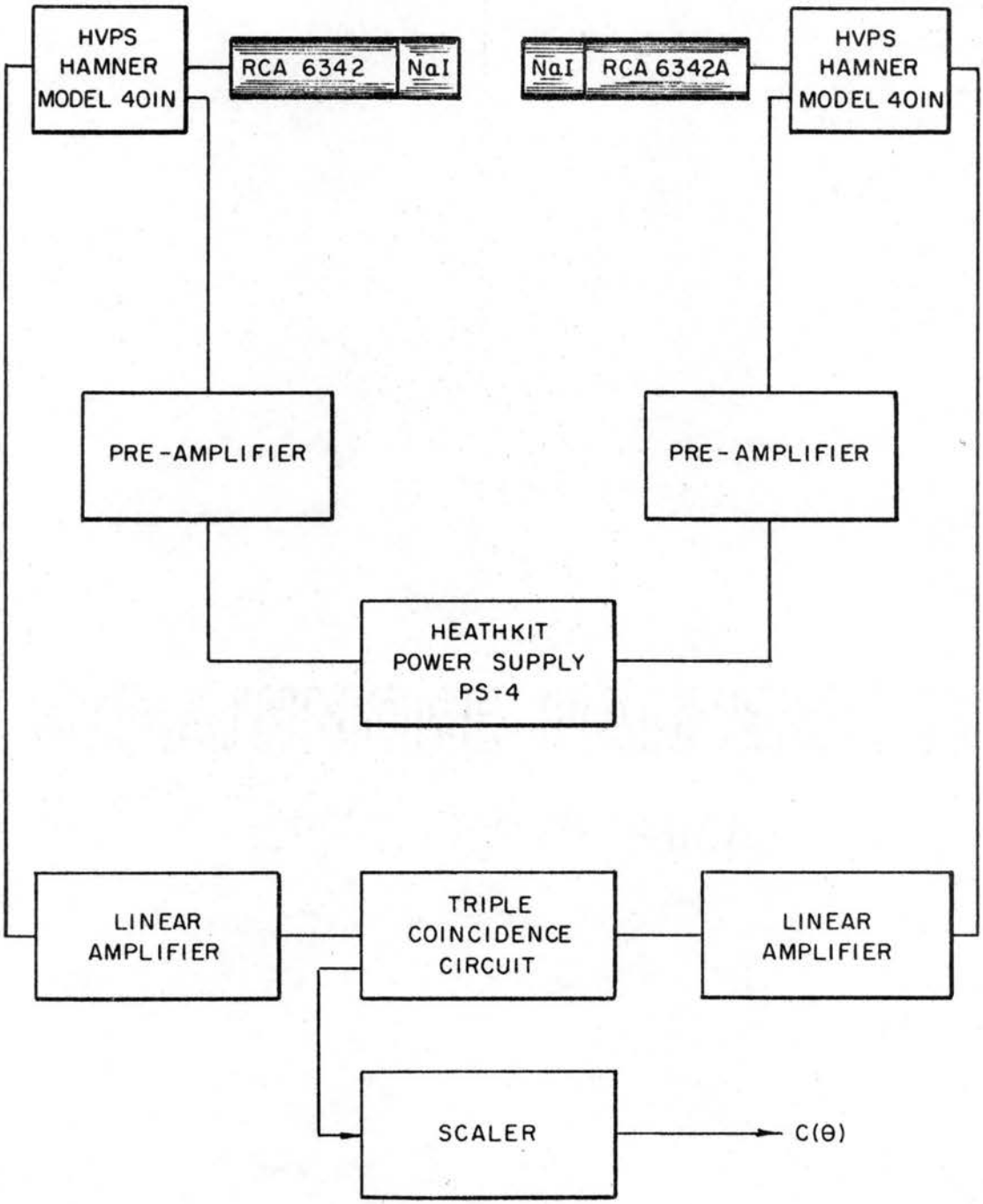

Figure 14. Block Diagram of the Angular Correlation Experiment

By a comparison with the theoretical values of A_2 and A_4 one can deduce the spin of the level.

Results and Discussion

Decay Scheme of Sb^{125}

The result of this work confirms the existing decay scheme which is shown in Figure 15. However, there is no clear evidence for the existence of the 0.401 Mev level. Table III gives the energies measured in this work compared to the results of others. For the angular correlation measurements, the result of the single spectrum confirms the absence of any impurities.

TABLE III

GAMMA-RAYS ENERGIES OF Te^{125} AFTER THE DECAY OF Sb^{125}

This Work E_{kev}	Lazar[19]	Narcisi[20]	Champion, et al[21] kev
109.44	109	109	---
176.45	176	176	172.4
(204.5, 208)	(203, 206)	(203, 206)	207.4
320.9	319	319	320.6
380.45	379	379	380.6
427.96	427	427	427.9
463.4	462	462	463.5
600.85	597	597	600.2
606.69	604	604	606.9
635.89	633	633	635.4
---	652	652	---
671.3	668	668	670.6

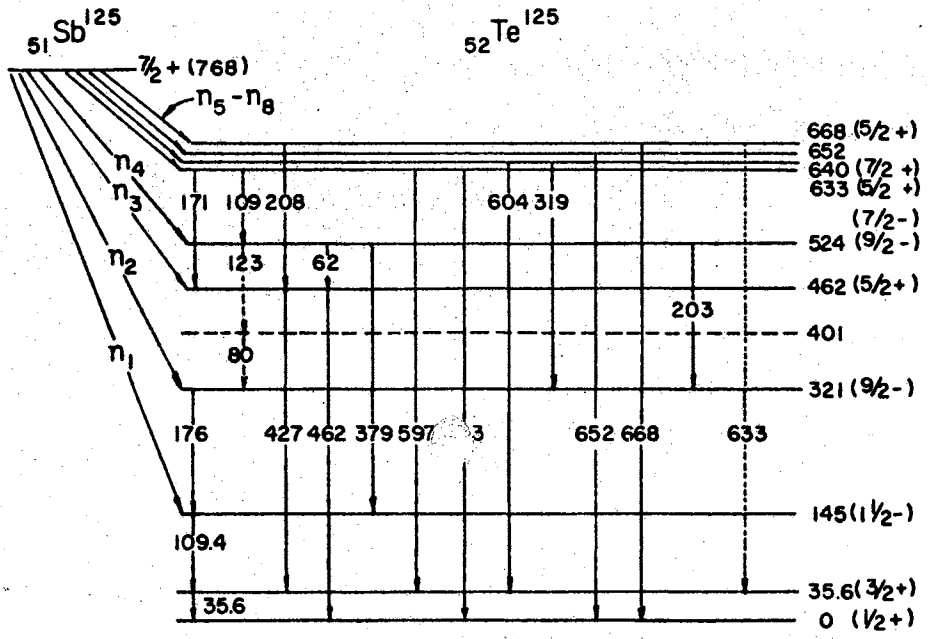

Figure 15. The Decay Scheme of Sb^{125}

Angular Correlation of γ-γ Cascade

The angular correlation set up has to be calibrated using a very well established standard. It is well known that the angular correlation between the 0.356 Mev and 0.082 Mev γ-γ cascade following the decay of Ba^{133} is quite well determined. The angular correlation function of this cascade was established to be[25]

$$W(\theta) = 1 + (0.042 \pm 0.005)\, P_2(\cos\theta) - (0.004 \pm 0.007)\, P_4(\cos\theta)$$

This angular correlation function has been re-established here as a check on the set up built to measure the angular correlation function of the 0.320 Mev - 0.176 Mev cascade in the Sb^{125} decay scheme. The result of the present set up for the 0.356 Mev - 0.082 Mev cascade in the Ba^{133} decay has been found to be:

$$W(\theta) = 1 + (0.0398 \pm 0.005)\, P_2(\cos\theta) - (0.0074 \pm 0.0095)\, P_4(\cos\theta)$$

with an anisotropy coefficient $A = 0.058 \pm 0.002$ where

$$A = \frac{W(\theta = \pi)}{W(\theta = \pi/2)} - 1, \text{ see Figure 16.}$$

<u>The angular correlation between 0.321 Mev - 0.176 Mev γ-γ cascade in the decay of Sb^{125}</u>

This was carried out specially to check the spin assignment of the 0.321 Mev level. The angular correlation function of this cascade turns out to be:

$$W(\theta) = 1 + (0.0532 \pm 0.002)P_2(\cos\theta) + (0.001 \pm 0.0003)\, P_4(\cos\theta)$$

with an anisotropy coefficient $A = 0.082 \pm 0.01$. Figure 17 shows W as a function of θ. From the F coefficients table[26] one finds that $A_2^{(1)}$, $A_4^{(1)} = 0.303$, 0.0 respectively where $A_2 = A_2^{(1)} A_2^{(2)}$ and

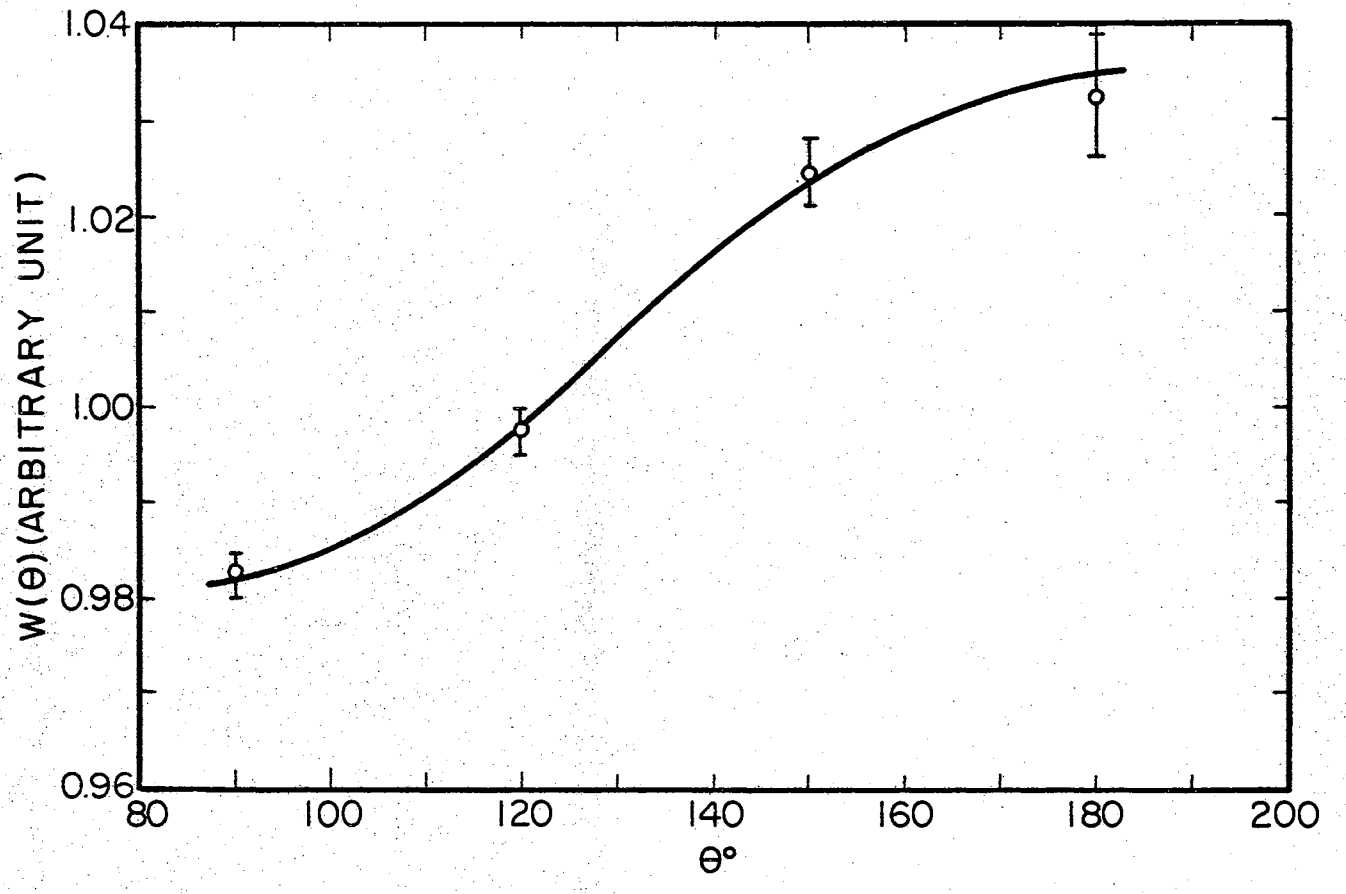

Figure 16. Angular Correlation between 0.356 Mev and 0.082 Mev Cascade in Cs^{133} after the Decay of Ba^{133}

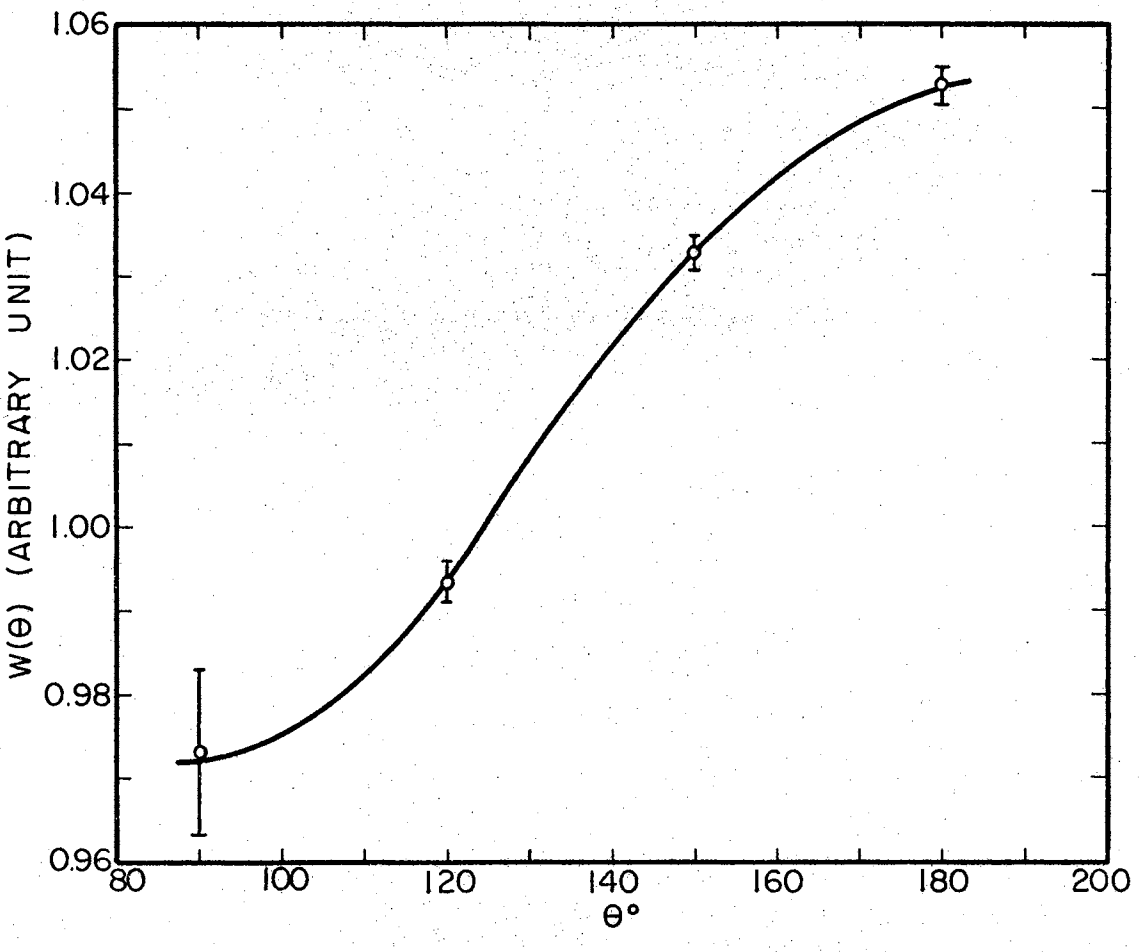

Figure 17. Angular Correlation between 0.321 Mev and 0.176 Mev Cascade in Te^{125} after the Decay of Sb^{125}

$A_4^{(1)}\ A_4^{(2)} = A_4$. Since $A_2 = 0.0532$ it follows that $A_2^{(2)} = 0.176$. From this result one can conclude that the cascade 0.321 Mev - 0.176 Mev has the $7/2^+$(D) $9/2^-$ (D.Q)$11/2^-$ sequence and supports the assignment of spin $9/2^-$ to the level 0.321 Mev, as was discussed by Narcisi[19] on the basis of his conversion coefficient measurements.

Conclusion

The measurement of the energies of Te^{125} following the decay of Sb^{125} shows no evidence of the 0.401 Mev level and the 0.652 Mev ground state transition, which was suspected by other workers, has not been observed, agreeing with the findings of Champion et al.[21] The angular correlation measurement of the 0.321 Mev - 0.176 cascade, however, supports the previous spin assignment of $9/2^-$ for the 0.321 Mev level.

Summary of Results and Conclusions

A comparison of the results of this work and those of other experimenters is given in Table IV. As far as the discrepancy in the reported results of Alvager et al and Knauf et al are concerned, this work confirms the findings of the latter. The theoretical estimate of Listengarten, which gives credence to the experimental work of reference[11], is not a serious limitation in accepting the current results because he uses a rather crude approximation in computing the actual ratio of the transition probabilities. The merit of his paper, however, is to point out the alternative interpretation of the observed double K-quanta coincidence as due to internal conversion of internal Compton effect. The upper limit for $\frac{W_{\gamma\gamma}}{W_\gamma}$ agrees more or less with the theoretical estimates of both reference[3] and reference[4]. At the

TABLE IV

SUMMARY OF THE RESULT AS COMPARED TO THE PREVIOUS WORKS

	Alvager et al[11]	This Work	Knauf et al[12]
$\frac{W_{e_k e_k}}{W_e + W}$	$4.5 \cdot 10^{-4}$	$\leq 0.75 \cdot 10^{-5}$	$0.66 \cdot 10^{-4}$
$\frac{W_{e_k e_k}}{W_\gamma}$	$2.44 \cdot 10^{-2}$	$\leq 4.1 \cdot 10^{-3} \pm 0.8$	$3.6 \cdot 10^{-3}$
$\frac{W_{kk}}{W_\gamma}$	$1.85 \cdot 10^{-2}$	$\leq 3.1 \cdot 10^{-3} \pm 0.6$	$2.7 \cdot 10^{-3}$
$\frac{W_{\gamma\gamma}}{W_\gamma}$	$8 \cdot 10^{-4}$	$\leq 3 \cdot 10^{-5}$	$2.2 \cdot 10^{-5}$

present stage of experimental investigation possible one can only determine the upper limits for the double quantum emission probability given above.

Measurement of the energies of the levels of Te^{125} shows no positive evidence for the existence of a new 0.401 level and angular correlation measurements confirm the spin of the 0.321 level as 9/2, odd parity.

REFERENCES

(1) Goppert-Mayer, M. Annalen Der Physik, 9, 273 (1931).

(2) Sachs, R. G. Physical Review, 57, 194 (1940).

(3) Eichler, J., and G. Jacob. Zeitschriff Fur Physik, 157, 286, (1959).

(4) Grechukin, D. P. Nuclear Physics, 62, 273 (1965).

(5) Mize, I. D., M. E. Bunker, and I. W. Starmer. Physical Review, 96, 444 (1954).

(6) Vanderleeden, J. C., and P. Jastram. Physics Letters, 19, 27 (1965).

(7) Church, E. L., and T. R. Gerholm. Physical Review, 143, 879 (1966).

(8) Nessin, M. AEC Report Cu(PNPL) - 207 (1960).

(9) Dell, G. F. Bull. Am. Phys. Soc. Ser. II6, 93 (1961).

(10) Alvager, T., H. Ryde, and P. Thieberger. Arkiv For Physik, 21, 559 (1962).

(11) Alvager, T., and H. Ryde. Arkiv For Physik, 17, 535 (1960).

(12) Knauf, K., H. Sommer, and H. Klewe-Nebenius. Zeitschrift Fur Physik, 197, 101 (1966).

(13) Shwinger, J. S., and J. R. Openheimer. Physical Review, 56, 1066 (1939).

(14) Listengarten, M. A. Vestnik Lenningrad University Ser. Fiz. ikim, 16, 142 (1962).

(15) Jacobson, A. M. Soviet Physics JETP, 2, 751 (1956).

(16) Vegors, S. H., Jr., L. L. Marsden, and R. L. Heath, IDO-16370, AEG Report.

(17) Chinglia, B., and R. Malvano. Nuclear Instruments and Methods, 45, 125 (1966).

(18) Biedenharn, L. C., and M. E. Rose. Reviews of Modern Physics, 25, 729 (1953).

(19) Narcisi, R. S. Harvard University, Department of Physics, Technical Report, No. 2-9 (April, 1959).

(20) Lazar, N. H. Physical Review, 102, 1058 (1959).

(21) Champion, P. to be published.

(22) Glendenning, N. K. Physical Review, 119, 213 (1960).

(23) Chandra, G. Proc. Ind. Acad. Sci., 46A, 360 (1957).

(24) Rose, M. Physical Review, 91, 610 (1953).

(25) Bodenstedt, E., H. J. Korner, and E. Mathias. Nuclear Physics, 11, 584 (1959).

(26) Rosenzweig, N., and P. Ferentz. Table of F Coefficients, A.N.L.R., ANAL-5324 (1955).

VITA

Ali A. Abdulla

Candidate for the Degree of

Doctor of Philosophy

Thesis: NUCLEAR SPECTROSCOPY STUDIES IN Xe^{131m} AND Sb^{125}

Major Field: Physics

Biographical:

Personal Data: Born July 1, 1939, in Khales, Iraq, the son of Morouah A. and A. Abdulla.

Education: Attended elementary school in Khales, Iraq; graduated from Baquba high school, Baquba, Iraq, in 1957; received the Bachelor of Science degree with a major in Physics from the University of Baghdad, Baghdad, Iraq, in 1961; received the Master of Science degree with a major in Physics from the University of Notre Dame, South Bend, Indiana, in 1964; completed the requirements for the Doctor of Philosophy degree in May, 1969.

Professional Experience: Was high school teacher from 1961-1962; graduate teaching assistant in Physics at Oklahoma State University, 1965-1968.

Organizations: Member of Sigma Pi Sigma